LINEAR TECHNOLOGY

# Journal of Analog Innovation

July 2015 Volume 25 Number 2

IN THIS ISSUE

4-phase supply supports 120A in tiny footprint 10

one driver is all you need for automotive LED headlight clusters 17

extend remote sensor battery life with thermal energy harvesting 24

simplify small solar systems with hysteretic controller 27

powering a Dust® mote from a piezo 29

# Op Amp Combines Femtoamp Bias Current with 4GHz Gain Bandwidth Product, Shines New Light on Photonics Applications

Glen Brisebois

Einstein published his seminal paper on the photoelectric effect 110 years ago, essentially inventing the discipline of photonics. One would think that over so many years the science and engineering surrounding photonics must have fully matured. But not so. Optical sensors—photodiodes, avalanche photodiodes, and photomultiplier tubes—continue to achieve astoundingly high dynamic ranges, enabling electronics to peer ever more deeply into the photonic world.

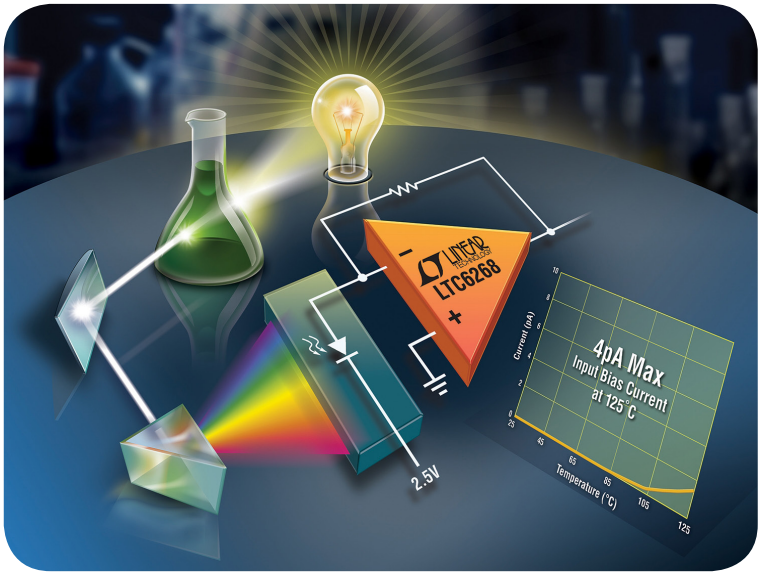


The LTC6268's performance meets the demands of the latest photonics applications.

Photosensors typically convert photons to electron current and are followed by a transimpedance function to transform the current into a voltage. The transimpedance function may be either a simple resistor or, for higher bandwidth, the summing node of an op amp, in which case it is called a transimpedance amplifier (TIA). The traditional enemies of the TIA are voltage noise, current noise, input capacitance, bias current and finite bandwidth. Enter the new LTC®6268-10 with 4.25nV/√Hz voltage noise, 0.005pA/√Hz current noise, a very low 0.45pF of input capacitance, 3fA of bias current and 4GHz of gain-bandwidth.

*(continued on page 4)*

# In this issue...


**COVER STORY**

Op Amp Combines Femtoamp Bias Current with 4GHz Gain Bandwidth Product, Shines New Light on Photonics Applications
**Glen Brisebois** 1

**DESIGN FEATURES**

4-Phase Power Supply Delivers 120A in Tiny Footprint, Features Ultralow DCR Sensing for High Efficiency
**Yingyi Yan, Haoran Wu and Jian Li** 10

3mm × 3mm Monolithic DC/DC Boost/Inverting Converters with 65V Power Switches
**Joshua Moore** 14

One LED Driver Is All You Need for Automotive LED Headlight Clusters
**Keith Szolusha and Kyle Lawrence** 17

**DESIGN IDEAS**

What's New with LTspice IV?
**Gabino Alonso** 22

Extend Remote Sensor Battery Life with Thermal Energy Harvesting
**Dave Salerno** 24

Simplify Small Solar Systems with Hysteretic Controller
**Mitchell Lee** 27

Powering a Dust Mote from a Piezoelectric Transducer
**Jim Drew** 29

new product briefs 31

back page circuits 32


# Linear in the News

## THE INDUSTRIAL INTERNET OF THINGS

Everywhere you turn, there is discussion around the emerging Internet of Things (IoT)—the concept that the Internet of the future will create a vast network of interconnected physical objects or "things" with embedded sensors, electronics and software. IoT devices are able to exchange data with other connected devices and human operators. According to industry analyst, Stifel, the IoT market today is already sizable, with an estimated 19.7 billion IoT devices deployed, and expected to grow to 95.5 billion devices deployed by 2025.

Much of the recent discussion about IoT revolves around "wearable technology"—Google glasses and Apple watches—but these applications are only part of a much larger IoT picture. There remains significant opportunity in the Industrial Internet of Things; analysts expect industrial to be one of the fastest growing IoT segments.

One major area of promise is to leverage real-time data gathered via wireless sensor networks (WSNs) to improve efficiency and streamline processes. Sensors can be placed in a broad range of environments, including buildings, city streets, bridges and tunnels, industrial plants, moving vehicles, or in remote locations such as along pipelines and weather stations. These applications require that WSNs draw extremely low power and yield wired-like reliability, often over a range of network architectures, sizes and data rates. Wireless mesh networks are increasingly popular because they can easily cover large areas using low power radios that reliably relay data from node to node.

Linear has developed expertise in this area via its Dust Networks® WSN product line. Linear's wireless sensor network products are suited for a wide range of Industrial IoT applications, including:

- Flow and process monitoring in industrial environments
- Data center energy management
- Fence line security
- Rail car preventive maintenance
- Smart street parking systems

## SOFTWARE DEVELOPMENT KIT ACCELERATES INDUSTRIAL IoT APPLICATION DEVELOPMENT

Linear Technology now offers a software development kit for the Industrial IoT. Linear Technology's SmartMesh IP™ wireless sensor networking products now provide the ability to program applications directly on the embedded ARM Cortex-M3, running Micrium's µC/OS-II real-time operating system. Application

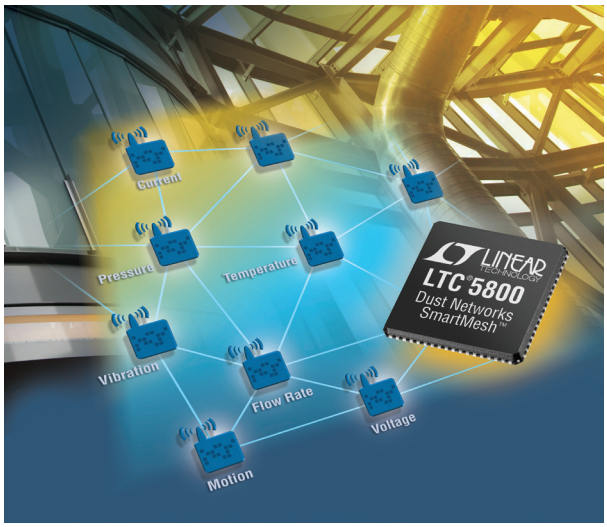


Linear's Dust Networks wireless sensor network products fuel applications in the Industrial Internet of Things.

development time is accelerated with a library of reference code and source code examples. Based on 6LoWPAN, SmartMesh IP mesh networking products include a pre-compiled networking stack that delivers >99.999% network reliability at ultralow power. This is particularly important for Industrial IoT applications, where wireless sensor networks may be deployed in harsh and remote environments, with little to no chance for maintenance. The On-Chip Software Development Kit (SDK) provided with the LTC5800-IPM (system-on-chip) and LTP™5901/2-IPM (PCB modules) is architected to ensure that developers can stably run both the pre-compiled SmartMesh IP networking stack and their applications simultaneously. For more information, see www.linear.com/solutions/5457.

## ENERGY HARVESTING AND IoT

The proliferation of wireless sensors supporting the Internet of Things has increased the demand for small, compact and efficient power converters tailored to untethered lower power devices. State-of-the-art and off-the-shelf energy harvesting (EH) technologies—for example, in vibration energy harvesting and indoor or wearable photovoltaic cells—yield power levels on the order of milliwatts under typical operating conditions. The operation of harvesting elements over several years makes them comparable to long-life primary batteries, both in terms of energy provision and the cost per energy unit. Systems incorporating EH are typically capable of recharging after depletion, something that systems powered by primary batteries cannot do. Most implementations use an ambient energy source as the primary power source, supplemented by a primary battery in case the ambient energy source goes away or is disrupted.

Linear Technology's LTC3331 is a complete regulating EH solution that delivers up to 50mA of continuous output current to extend battery life when harvestable energy is available. It requires no supply current from the battery when providing regulated power to the load from harvested energy and only 950nA operating when powered from the battery under no-load conditions. The LTC3331 integrates a high voltage EH power supply, plus a synchronous buck-boost DC/DC converter powered from a rechargeable primary cell battery to create a single non-interruptible output for energy harvesting applications such as those in wireless sensor networks. Another device, the LTC3388-1/-3, is a 20V input-capable synchronous buck converter that delivers up to 50mA of continuous output current and operates from an input voltage range of 2.7V to 20V, ideal for a wide range of energy harvesting and IoT battery-powered applications including "keep-alive" sensor and industrial control power.

## AWARDS

The LTC2000 16-bit, 2Gsps DAC received the 2014 Product Award from 21ic.com in China.

## CONFERENCES & EVENTS

**IEEE Nuclear and Space Radiation Effects Conference, Marriott Copley Place, Boston, Massachusetts, July 13–17, Booths 8 & 9—** Linear is showcasing its products for space and harsh environments. More info at www.nsrec.com

**2nd Dust Networks Consortium, Tokyo Conference Center, Tokyo, Japan, July 21—**Software and device vendors, integrators and monitoring service providers are invited to learn about wireless sensor network system capabilities. More info at www.dust-consortium.jp/

**The Battery Show/Electric & Hybrid Vehicle Tech Expo, Suburban Collection Showplace, Novi, Michigan, September 15–17—**Presenting Linear's battery management system products. More info at www.thebatteryshow.com/

**IoT World Congress, Gran Via Venue, Barcelona, Spain, September 16–18—**Linear will highlight its Dust Networks wireless sensor network products. More info at www.IoTsworldcongress.com/en/home

**Sensors & Instrumentation for Test, Measurement & Control, The National Exhibition Centre, Birmingham, UK, September 30 to October 1—**Linear will showcase products and solutions related to wireless sensor networks. More info at www.sensorsandinstrumentation.co.uk/ ■

The calculated CV + I noise for the LTC6268-10 at 1MHz is 0.052pA/√Hz, compared to 0.156pA/√Hz for the OPA657; a factor of three better for the LTC6268-10.

*(LTC6268, continued from page 1)*

## UNDERSTANDING VOLTAGE NOISE AND CURRENT NOISE CONTRIBUTIONS IN TIAs

Output noise in TIAs is a result of combined input voltage noise and input current noise. This combined effect is often specified as a current noise referred to the input—essentially the output voltage noise divided by the gain in ohms—but it actually arises from both input noise sources. In fact, the dominant cause of output noise is usually input voltage noise (Figure 1).

By virtue of feedback, the minus input is fixed at virtual ground so the current noise $i_n$ passes directly through $R_F$ and contributes to total current noise with a factor of 1. Also by virtue of feedback, the voltage noise $e_n$ is placed in parallel with the input capacitance $C_{IN}$ and induces a current noise of $e_n/Z(C_{IN})$. The impedance of a capacitor is $1/2\pi fC$, so the effective current noise due to input voltage noise and capacitance is $2\pi fC_{IN}e_n$. So the total op amp noise (ignoring $R_F$ thermal noise) is

$$I_{NOISE} = \sqrt{(2\pi fC_{IN}e_n)^2 + (i_n)^2}$$

This is sometimes referred to as CV + I noise and makes an excellent figure of merit for an op amp, because it incorporates only op amp characteristics, neglecting external aspects of the circuit such as photosensor capacitance and $R_F$ thermal noise. It is essentially the best the op amp can do.

**Figure 1. The op amp with its noise sources and input capacitance. Total op amp noise (ignoring $R_F$ thermal noise) is $I_{NOISE} = i_n + 2\pi fC_{IN}e_n$ (added rms-wise).**

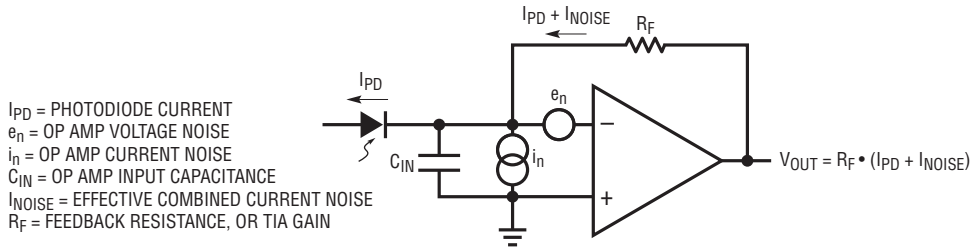


## SAMPLE CALCULATION AND COMPARISON BETWEEN LTC6268-10 AND COMPETITIVE OPA657

The CV + I noise is a useful figure of merit for comparing op amps, but it does have a dependency on frequency. An insightful comparison can be made by initially comparing them at a specific frequency and then observing the differences in the plots of CV + I noise versus frequency that inevitably arise. For example, let's compare the LTC6268-10 and competitive OPA657 by starting with a calculation at 1MHz.

**Figure 2. CV + I current noise versus frequency for the LTC6268-10 and OPA657. The LTC6268-10 is considerably quieter.**

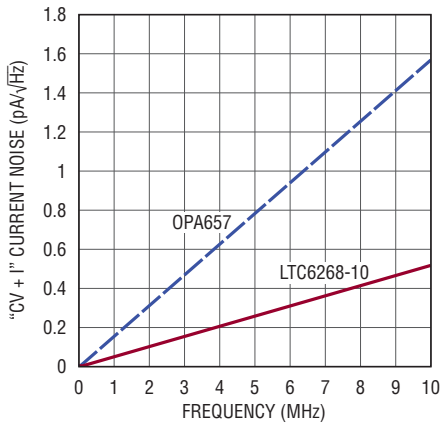


The LTC6268-10 data sheet gives plots of current noise versus frequency showing 0.05pA/√Hz at 1MHz, and of voltage noise versus frequency showing 4nV/√Hz at 1MHz. Using the input capacitance of 0.55pF (0.45pF for CCM, plus 0.1pF for CDM), the total CV noise at 1MHz can be calculated as

$$\text{CV NOISE} = 2\pi \bullet 1\text{MHz} \bullet 0.55\text{pF} \bullet 4\text{nV}/\sqrt{\text{Hz}}$$
$$= 0.014\text{pA}/\sqrt{\text{Hz}}$$

Summing this rms-wise with the native I noise of 0.05pA/√Hz, we get 0.052pA/√Hz of total CV + I noise at 1MHz.

The same calculation for the competitive OPA657 can also be performed. It specifies 4.8nV/√Hz voltage noise, 5.2pF input capacitance (4.5pF for $C_{CM}$ plus 0.7pF for $C_{DM}$), and 1.3fA/√Hz current noise. Calculating total CV + I noise gives 0.156pA/√Hz at 1MHz for the OPA657, about three times worse than LTC6268-10.

Figure 2 shows a plot of CV + I noise for LTC6268-10 and OPA657 versus frequency. The reason the LTC6268-10 outperforms the OPA657 is its lower voltage noise and its much lower input capacitance. And

A powerful method to reduce feedback capacitance is to shield the E field paths that give rise to the capacitance. In this particular case, the method is to place a ground trace between the resistor pads. Such a ground trace shields the output field from getting to the summing node end of the resistor, effectively shunting the field to ground instead.

because the LTC6268-10 has lower voltage noise, it continues to outperform the OPA657 as the sensor capacitance is added and increased. Furthermore, the LTC6268-10 features a rail-to-rail output and can operate on a single 5V supply, burning half the power of OPA657.

### GAIN BANDWIDTH, AND ACHIEVING HIGH BANDWIDTH AT HIGH IMPEDANCE

Another advantage of the LTC6268-10 is its serious 4GHz gain bandwidth product. In fact, you'll find that the LTC6268-10 is able to find and use tiny parasitic capacitances that other op amps miss. Normally, high value resistors begin to reduce their net impedance at high frequency due to their end-to-end capacitance. The key to exploiting the 4GHz gain bandwidth of the LTC6268-10 with higher gain TIAs is to minimize the feedback capacitance around the main feedback resistor. Though minimized, the LTC6268-10 can use the tiny residue feedback capacitance to compensate the feedback loop, extending resistor bandwidth to several MHz. Following is a design example at 402k.

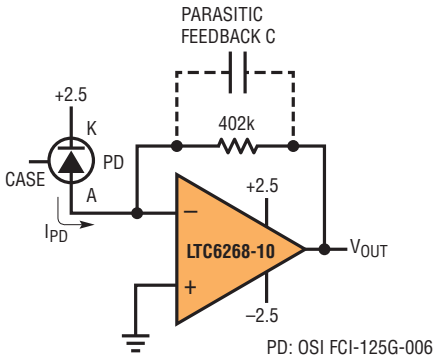


Figure 3. LTC6268-10 and low capacitance photodiode in a 402kΩ TIA

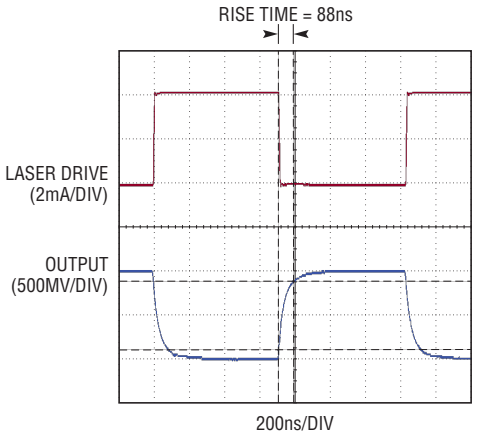


Figure 4. Time domain response of 402kΩ TIA without extra effort to reduce feedback capacitance. Rise time Is 88ns and BW is 4MHz.

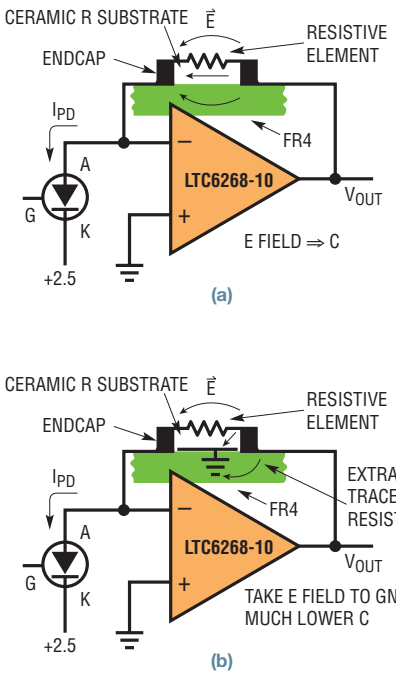


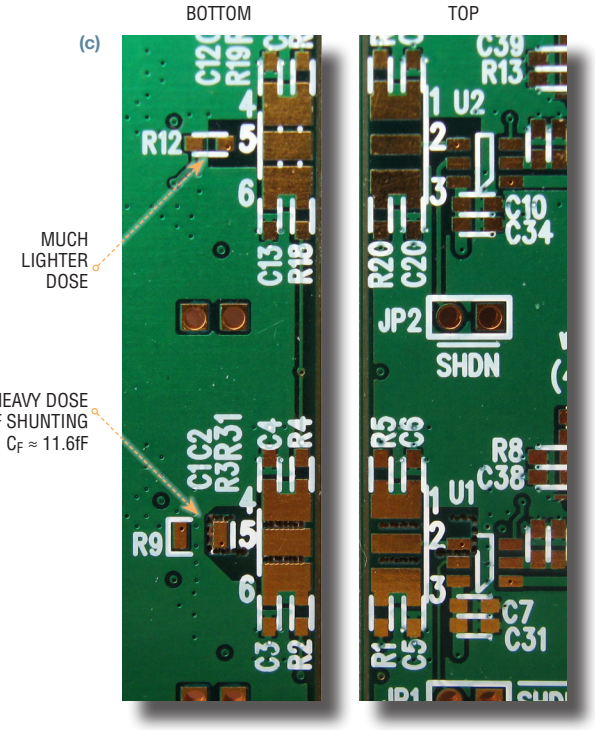


Figure 5. A normal layout (a) and a field-shunting layout (b). Circuit board in (c) shows actual layout with extra shunting at R9, less at R12. Simply adding a ground trace under the feedback resistor does much to shunt field away from the feedback side, dumping it to ground. Note that the dielectric constant of FR4 and ceramic is typically 5, so most of the capacitance is in the solids and not through the air. Such field shunting techniques reduced feedback capacitance from approximately 100fF in Figure 4 to 11.6fF in Figure 6. Note also that the feedback trace is exposed in upper (c) but entirely shielded in lower (c).

Bandwidth and rise time went from 4MHz (88ns) to 34MHz (10.3ns), a factor of 8. The ground trace used for LTC6268-10 was much wider than that used in the case of the LTC6268, extending under the entire resistor dielectric.

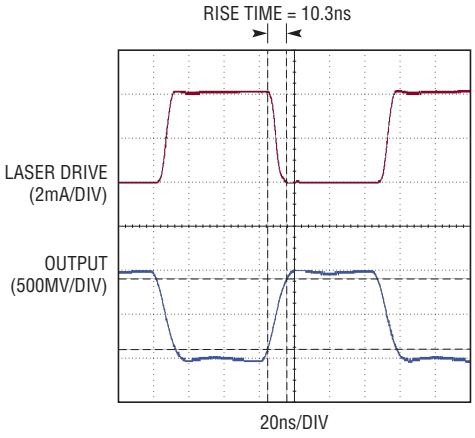


**Figure 6. LTC6268-10 in a 402kΩ TIA with extra layout effort to reduce feedback capacitance achieves 10.3ns total system rise time, or 34MHz total system bandwidth. This is an 8x increase in bandwidth, due to a well placed bit of ground trace.**

Good layout practices are essential to achieving best results from a TIA circuit. The following two examples show drastically different results from an LTC6268-10 in a 402k TIA (Figure 3). The first example is with an 0805 resistor in a basic circuit layout. In a simple layout, without expending a lot of effort to reduce feedback capacitance, the rise time achieved is about 88ns (Figure 4), implying a bandwidth of 4MHz (BW = 0.35/$t_R$). In this case, the bandwidth of the TIA is limited not by the GBW of the LTC6268-10, but rather by the fact that the feedback capacitance is reducing the actual feedback impedance (the TIA gain itself) of the TIA. Basically, it's a resistor bandwidth limitation. The impedance of the 402k is reduced by its own parasitic capacitance at high frequency. From the 4MHz bandwidth and the 402k low frequency gain, we can estimate the total feedback capacitance as

$$C_F = \frac{1}{2\pi \bullet 4MHz \bullet 402k} = 0.1pF$$

That's fairly low, but it can be reduced further, maybe much further.

With some extra layout techniques to reduce feedback capacitance, the bandwidth can be increased. Note that we are increasing the effective "bandwidth" of the 402k resistance. A very powerful method to reduce feedback capacitance is to shield the E field paths that give rise to the capacitance. In this case, the method is to place a ground trace between the resistor pads. Such a ground trace shields the output field from getting to the summing node end of the resistor, effectively shunting the field to ground instead. The trace increases the output load capacitance very slightly. See Figure 5a and 5b for a pictorial representation, and Figure 5c for an example layout.

Figure 6 shows the dramatic increase in bandwidth simply by careful attention to low capacitance methods around the feedback resistance. Bandwidth and rise time went from 4MHz (88ns) to 34MHz (10.3ns), a factor of 8. The ground shield trace used for the LTC6268-10 was much wider than that used in the high speed case of the LTC6268 (see LTC6268 data sheet), extending under the entire resistor dielectric. Assuming all the bandwidth limit is due to feedback capacitance (which isn't fair), we can calculate an upper limit of

**Figure 7. A photograph and x-ray of a Hamamatsu photomultiplier tube. The electronics components visible at right are the encapsulated high voltage supply. (Do not x-ray your PMT unless it is already unusable.)**

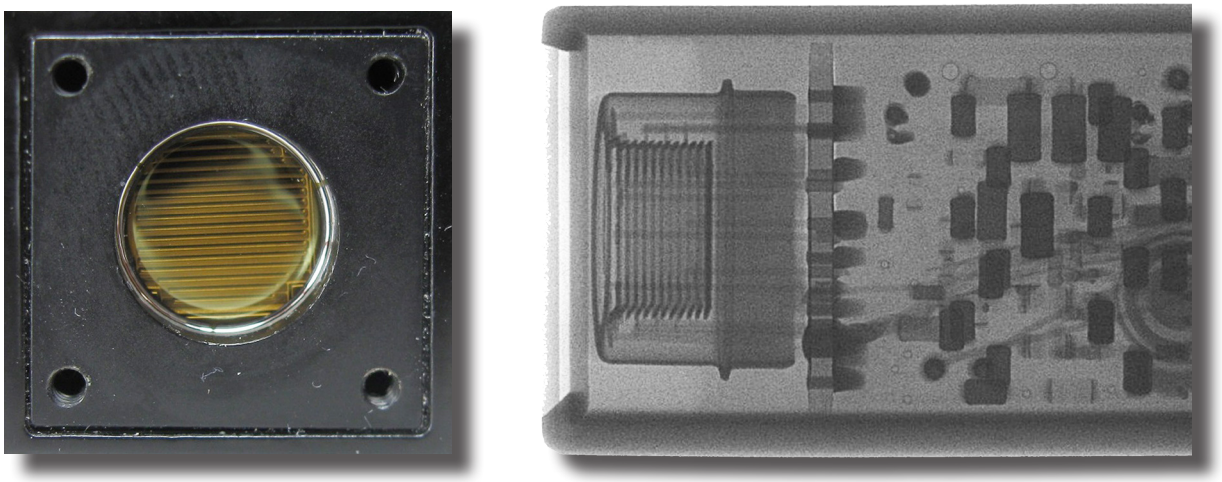

Photomultiplier tubes yield photonics gains above one million, meriting their considerably high cost. Given the high inherent gain, the TIA gain can be reduced, and bandwidth extended to the point that single photon events can be isolated. When using the LTC6268-10 at low gain, however, care must be taken to ensure its gain stability requirement of 10 is met, or there is risk of oscillation.

$$C_F = \frac{1}{2\pi \bullet 34MHz \bullet 402k} = 11.6fF$$

## A PHOTOMULTIPLIER TUBE (PMT) AT LOWER IMPEDANCE

Photomultiplier tubes (photograph and x-ray shown in Figure 7) yield photonics gains above one million, meriting their considerably high cost. Given the high inherent gain, the TIA gain can be reduced, and bandwidth extended to the point that single photon events can be isolated. One convenient feature of a PMT is self-excitation, drawing energy either from local cosmic radiation or its own thermionic electron emission when the plate voltage is high, producing a random Dirac-delta-like ping of electrons on the output plate.

When using the LTC6268-10 at low gain, however, care must be taken to ensure its gain stability requirement of 10 is met, or there is risk of oscillation. The Hamamatsu PMT did not have a specified output plate capacitance, but the HP4192 impedance analyzer measured it to be 10pF at its maximum test frequency of 13MHz. Given that fact, a feedback capacitance of 1pF should have been adequate to ensure an apparent noise gain of 11.

However, the pins on the PMT were about 3/4 inch long (Figure 8), and with the LTC6268-10 connected to it in a gain of

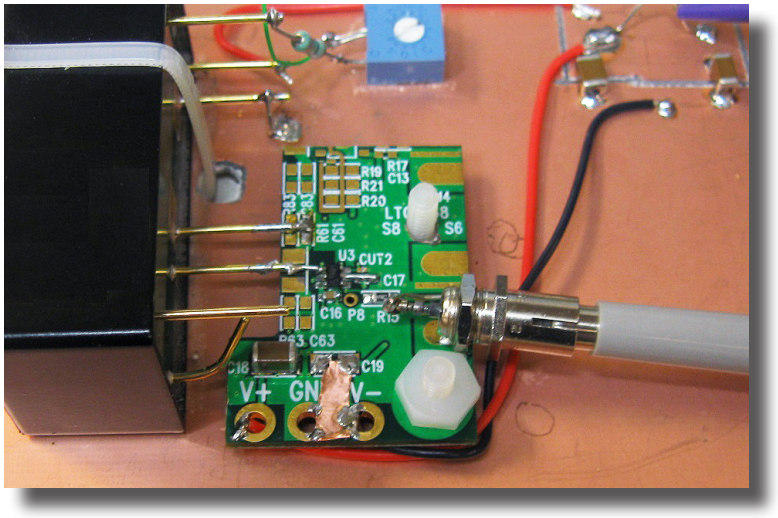


Figure 8. First attempt at connecting LTC6268-10 to PMT output plate. Note the 3/4-inch or so transmission line created by the PMT plate pin. That's far below 1/4-lambda at 300MHz. What could possibly go wrong? See Figure 9.

Figure 9. The transmission line was short compared to a 300MHz assessment, but long enough to be a problem when compared to real bandwidth available.

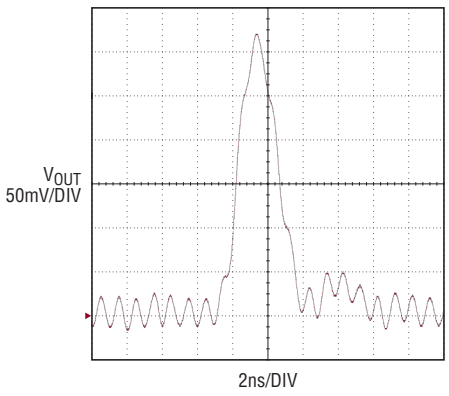


Figure 10. Much tighter design on dedicated board. LTC6268-10 is now much closer to the PMT body and therefore the PMT output plate capacitance. Transmission line still exists, but it is hanging midair and is not "in the way."

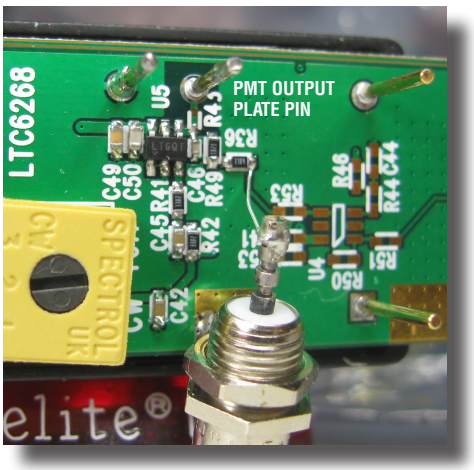


Figure 11. Reducing the transmission line length is key to achieveing good results. Output pulse half-width is 2.2ns. Exact –3dB bandwidth is not as relevant as a clean time-domain response.

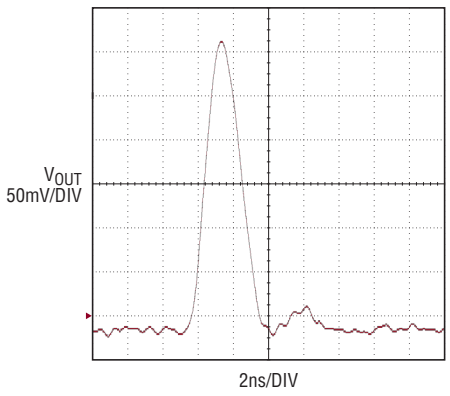

The LTC6268 achieves bias currents two orders of magnitude lower than any previous Linear Technology amplifier, which requires accurately measuring femtoamps—while measuring picoamps is challenging enough.

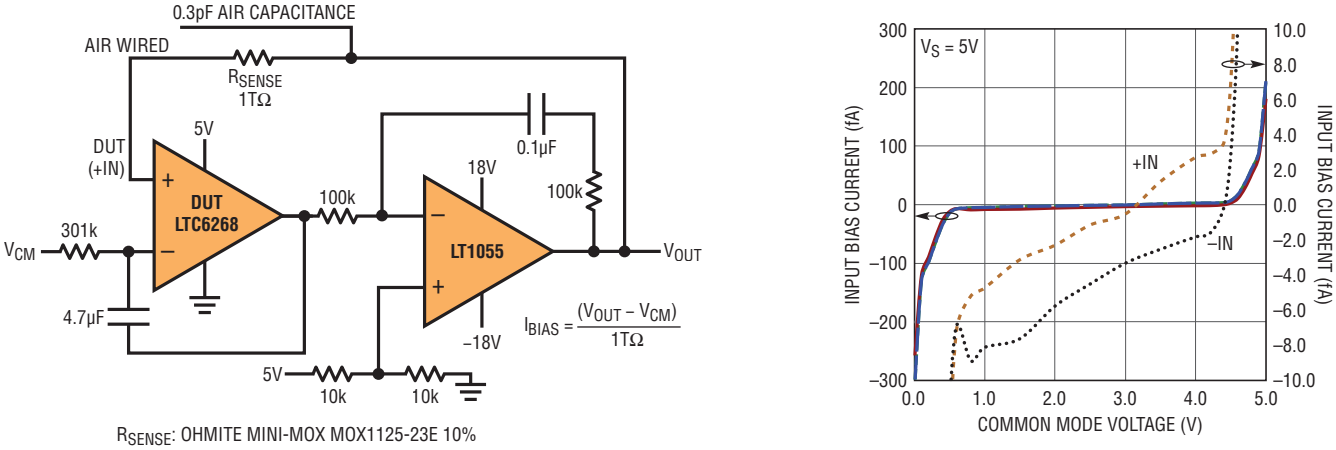


**Figure 12. Circuit for measuring femtoamp bias current of LTC6268 (the unity gain stable version of LTC6268-10) and measured results, at various common modes.**

1.82k, a sustained oscillation of 1.05GHz became apparent alongside the expected response to a dark-current ping (Figure 9). Trying a variety of feedback capacitors between 0.2pF and 1pF around the LTC6268-10 did not help. The conclusion was that the short transmission line was changing the appearance of the 10pF plate at high frequency, and was therefore not satisfying the gain of 10 requirement.

With the LTC6268-10 positioned closer to the PMT body on a new board (Figure 10), the oscillation was quenched and the much improved response of Figure 11 was achieved. Component feedback capacitance installed was 0.8pF (Murata GJM1555C1HR80). Another change on the board was that the feedback resistor was brought to the topside, eliminating two vias.

## MEASURING FEMTOAMPS

The LTC6268 achieves bias currents about two orders of magnitude lower than any previous Linear Technology amplifier, which requires accurately measuring femtoamps—while measuring picoamps is challenging enough. In production testing, speed is of the essence, so capacitive switching techniques are employed. In our tests made on the bench, where speed is not an issue, a sense resistor was preferred.

Assuming a 1mV op amp offset allowance (actually 0.7mV max), and a desired resolution of 1fA, the required sense resistor comes to 1mV/1fA = 1TΩ. Fortunately, Ohmite makes a 1T resistor, in the long blue MOX1125 package. In order to measure input bias current at various input common mode voltrage levels to the DUT (device under test), the circuit of Figure 12 was employed.

Circuit board effects were removed by removing the circuit board. That is, removing the board under the LTC6268 noninverting input and whisker connecting it through air to the 1TΩ resistor. This leaves just the op amp pin, the resistor and their package materials in place, hanging midair, as you can see in Figures 13 (topside) and 14 (bottom side).

Figure 15 shows the time domain response, settling well in 2.2 seconds. The overshoot isn't actually overshoot in the conventional sense, but rather the charge necessary to move the total input C, effectively looking like a short term bias current. The voltage delta of the overshoot is about 190mV, and extends about 1.25 seconds in width.

The total charge can be estimated by calculating the area of the triangle created by the voltage-overshoot in Figure 15:

$$\text{TOTAL CHARGE} = \frac{\frac{1}{2} \bullet 190\text{mV} \bullet 1.25\text{s}}{1\text{T}\Omega} = 0.12\text{pC}$$

With Q = CV, and a 200mV step, the total input C can be calculated as

The LTC6268-10 features extremely low 4.25nV/√Hz voltage noise, 0.005pA/√Hz current noise, a very low 0.43pF of input capacitance, 3fA of bias current and 4GHz of gain-bandwidth.

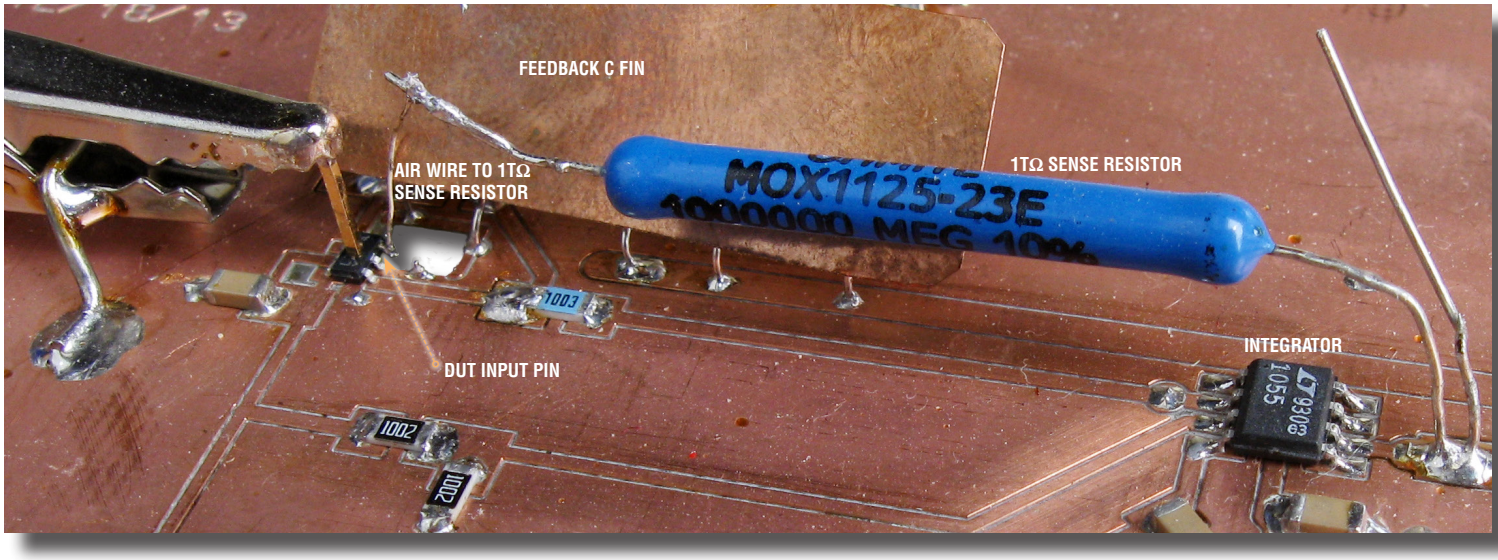


Figure 13. Actual board implementation of the femtoamp measurement board. Note the placement respecting the long blue resistor. Feedback capacitance to DUT input pin is through-air only.

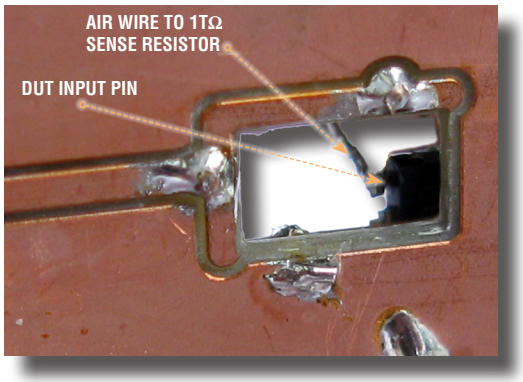


Figure 14. The bottom side of the board, showing the DUT input pin hanging midair.

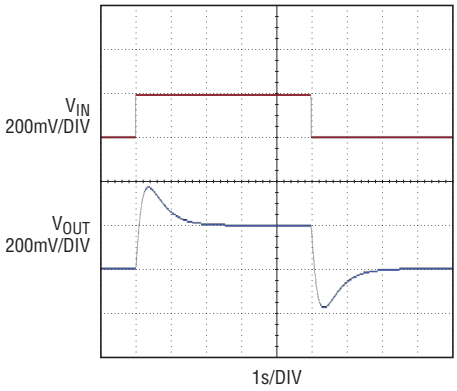


Figure 15. Time domain response. Settles in 2.2 seconds with a 200mV change in common mode voltage. Overshoot is real, as the teraohm resistor moves the voltage on the 0.6pF total input capacitance.

Q/V = 0.6pF. A rough allocation would be 0.45pF for the LTC6268 input $C_{DM}$ and another 0.15pF for the whisker and resistor lead. Output noise was measured at just under $1mV_{P-P}$, consistent with the objective of resolving 1fA.

## CONCLUSION

The LTC6268-10 significantly reduces the traditional enemies of TIAs: voltage noise, current noise, input capacitance and bias current. It features extremely low 4.25nV/√Hz voltage noise, 0.005pA/√Hz current noise, a very low 0.43pF of input capacitance, 3fA of bias current and 4GHz of gain-bandwidth. ■

# 4-Phase Power Supply Delivers 120A in Tiny Footprint, Features Ultralow DCR Sensing for High Efficiency

**Yingyi Yan, Haoran Wu and Jian Li**

The LTC3875 is a feature-rich dual-output synchronous buck controller that meets the power density demands of modern high speed, high capacity data processing systems, telecom systems, industrial equipment and DC power distribution systems. The LTC3875 delivers high efficiency with reliable current mode control, ultralow DCR sensing and strong integrated drivers in a 6mm × 6mm 40-pin QFN. Multiple LTC3875s can be paralleled to provide higher current, or it can be combined with the LTC3874 to deliver the same performance with a smaller footprint.

The LTC3874 is a small footprint (4mm × 5mm QFN), dual PolyPhase® current mode synchronous step-down slave controller (phase extender). It is suitable for high current, multiphase applications when paired with a companion master controller, such as LTC3875. The LTC3874 can use sub-milliohm DC resistance power inductors to optimize efficiency. Immediate response to system faults guarantees reliability of the total solution.

## 1V $V_{OUT}$, 120A CONVERTER WITH PARALLEL LTC3875s

The LTC3875 can be easily configured as dual-phase, single-output operation for high current outputs. This design can be expanded with more converters and phases in parallel for even higher current. Figure 1 shows a 4.5V~14V input, single-output application schematic using two LTC3875s. The LTC3875s' four channels run with 90° phase shift, reducing input RMS current ripple and required capacitor size.

Figure 1. A single-output, 4-phase (1.0V/120A) converter

Each phase supports 30A of current with one top MOSFET and one bottom MOSFET.

The LTC3875 employs a unique current sensing architecture to enhance its signal-to-noise ratio, enabling current mode control even with a small sense signal from a very low inductor DCR—1mΩ or less. As a result, efficiency is high and jitter is low. Current mode control yields fast cycle-by-cycle current limit, current sharing and easy feedback compensation.

The LTC3875 can sense a DCR value as low as 0.2mΩ with careful PCB layout. The LTC3875 uses two positive sense pins SNSD+ and SNSA+ to acquire signals. The filter time constant of the SNSD+ should match the L/DCR of the output inductor, while the filter at SNSA+ should have a bandwidth five times larger than that of SNSD+. Moreover, an

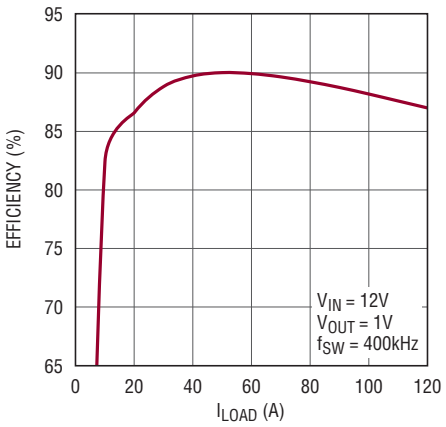


Figure 2. Efficiency of circuit in Figure 1

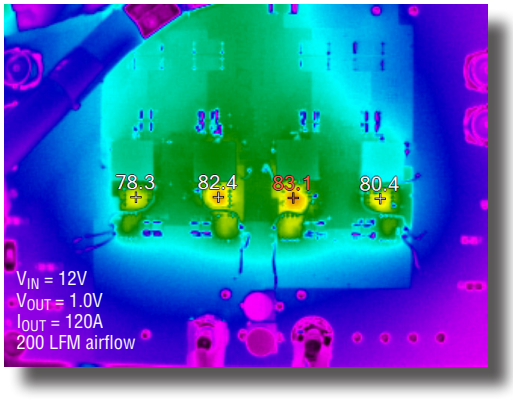


Figure 3. Thermal scan of 4-channel regulator

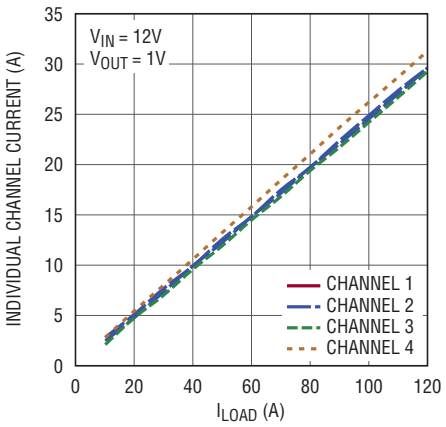


Figure 4. DC current sharing is balanced among the four channels, even at very high current loads

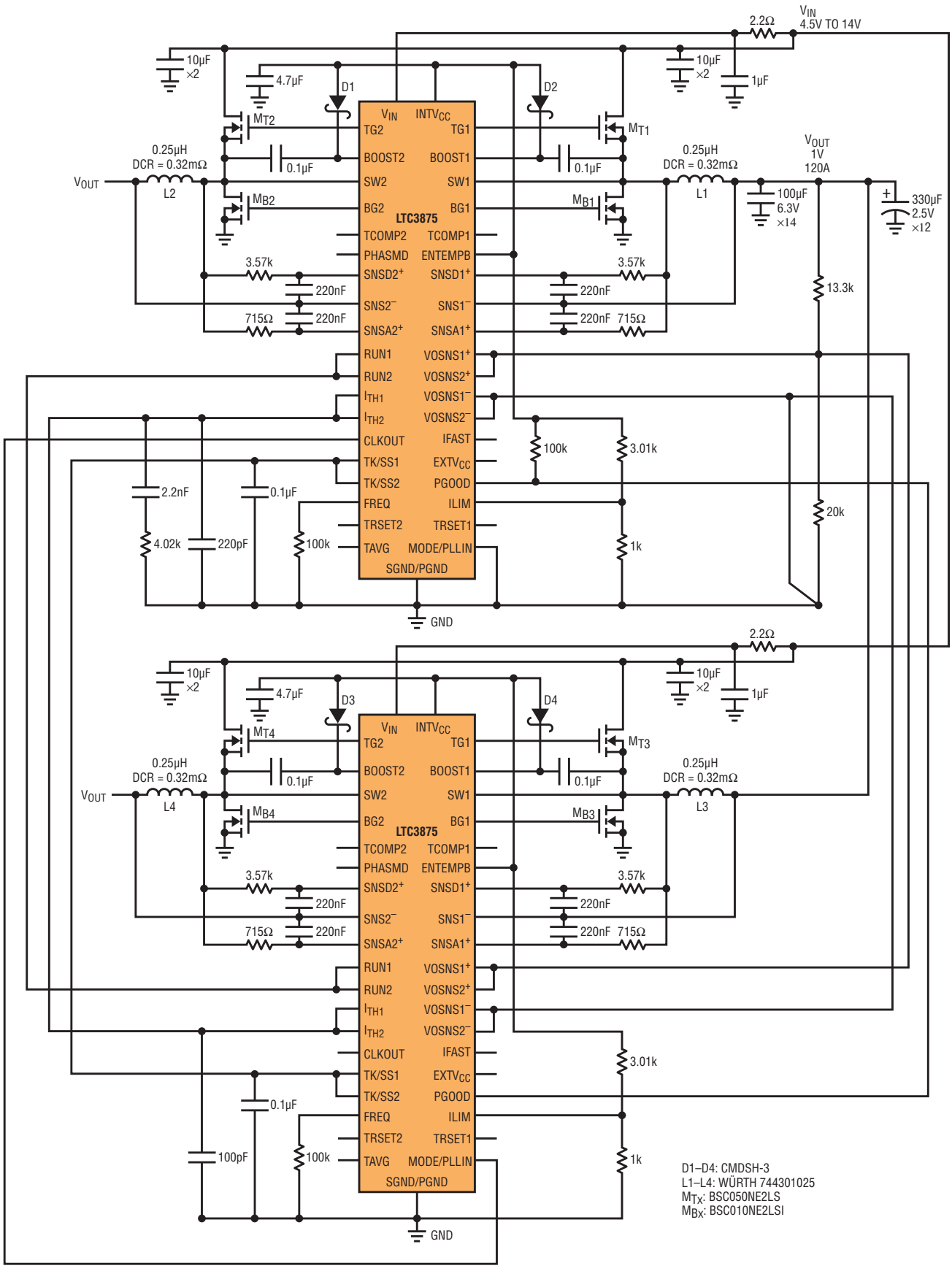
VIN
4.5V TO 14V
2.2Ω
10µF
×2
4.7µF
D1
D2
1µF
MT2
MT1
0.25µH
DCR = 0.32mΩ
0.1µF
VOUT
1V
120A
L2
L1
MB2
MB1
100µF
6.3V
×14
330µF
2.5V
×12
LTC3875
VIN
INTVCC
TG2
TG1
BOOST2
BOOST1
SW2
SW1
BG2
BG1
TCOMP2
TCOMP1
PHASMD
ENTEMPB
SNSD2+
SNSD1+
SNS2−
SNS1−
SNSA2+
SNSA1+
RUN1
RUN2
ITH1
ITH2
VOSNS1+
VOSNS2+
VOSNS1−
VOSNS2−
CLKOUT
IFAST
TK/SS1
TK/SS2
EXTVCC
PGOOD
FREQ
ILIM
TRSET2
TRSET1
TAVG
MODE/PLLIN
SGND/PGND
3.57k
220nF
715Ω
13.3k
100k
3.01k
20k
2.2nF
4.02k
220pF
1k
GND
D3
D4
MT4
MT3
MB4
MB3
L4
L3
100pF
D1–D4: CMDSH-3
L1–L4: WÜRTH 744301025
MTX: BSC050NE2LS
MBX: BSC010NE2LSI

Figure 5. A single-output, 4-phase (1.0V/120A) converter featuring LTC3875 and LTC3874

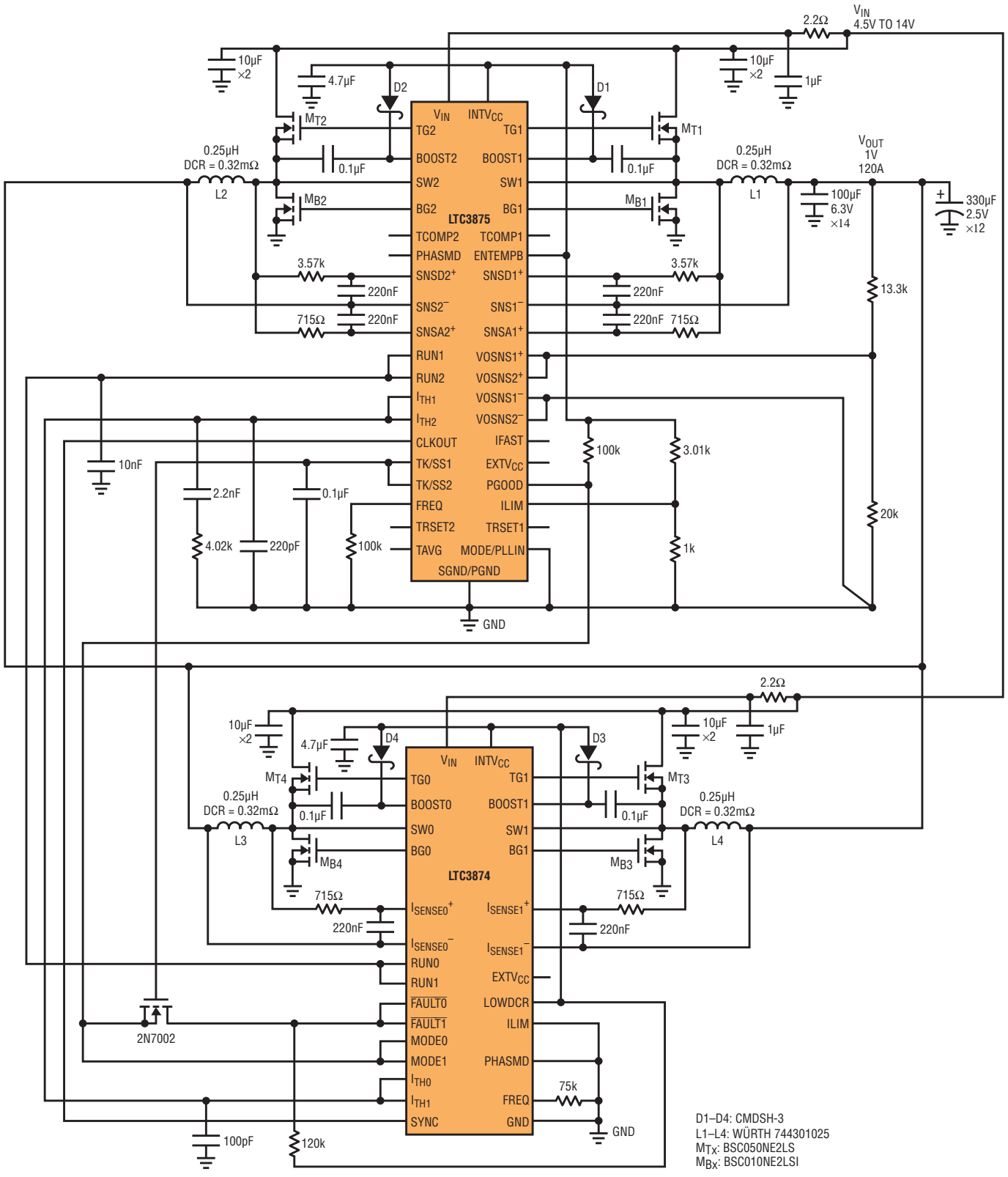

The LTC3875 delivers an outsized set of features for its small 6mm × 6mm 40-pin QFN. It offers high efficiency with reliable current mode control, ultralow DCR sensing and strong integrated drivers. Tracking, multichip operation, and external sync capability fill out its menu of features.

additional temperature compensation circuit can be used to guarantee the accurate current limit over a wide temperature range, and DCR variation.

Efficiency can be optimized with an ultralow DCR inductor. As shown in Figure 2, the total solution efficiency in forced continuous mode (CCM) is 87.1% at 12V input and 1.0V, 120A output. The hot spot (bottom MOSFET) temperature rise is 58.1°C with 200 LFM airflow as shown in Figure 3, where the ambient temperature is about 25°C.

The DC current sharing among the four channels is shown in Figure 4. The difference at full load is about 2.0A (±3.5%) with a 0.32mΩ DCR inductor.

### THE LTC3874 SLAVE CONTROLLER REDUCES SOLUTION SIZE AND COMPONENT COUNT IN ALTERNATE 1V, 120A CONVERTER

Figure 5 shows an alternative to the 4.5V~14V input, single-output application shown in Figure 1—in this case using an LTC3875 and an LTC3874. The LTC3874 phase extender acts as a slave controller, but it supports all the programmable features as well as fault protection.

- $I_{TH}$ pins of the LTC3875 and LTC3874 are connected for current sharing.
- The CLKOUT pin of the LTC3875 is connected to the SYNC pin of the LTC3874 to synchronize switching frequency.
- The MODE pin of the LTC3874 is connected to PGOOD, which allows DCM operation during start-up period for pre-bias load condition.
- The FAULT pin of the LTC3874 is pulled up to the INTVCC pin and is connected to the PGOOD pin of LTC3875 via a TK/SS pin voltage-controlled MOSFET. When the PGOOD pin is pulled low due to a fault, the LTC3874 can shut down both channels for protection purposes.

Like the LTC3875, the LTC3874's current mode control is accurate even with sense signals from an inductor DCR below 1mΩ. Compared to the master LTC3875, the LTC3874 simplifies pinout and uses only one set of RC components for DCR current sensing. The filter time constant of the RC filter should have a bandwidth five times larger than that of the L/DCR of the output inductor.

The total solution efficiency and thermal performance is similar to that of the two-LTC3875 solution. The DC current sharing among four channels is accurate. The difference at full load is about 1.6A with a 0.32mΩ DCR inductor.

### CONCLUSION

The LTC3875 delivers an outsized set of features for its small 6mm × 6mm 40-pin QFN. It offers high efficiency with reliable current mode control, ultralow DCR sensing and strong integrated drivers. Tracking, multichip operation, and external sync capability fill out its menu of features. Furthermore, the slave controller LTC3874 offers a smaller footprint solution when paired with the LTC3875. The LTC3875 and LTC3874 are ideal for high current applications, such as telecom and datacom systems, industrial and computer systems applications. ■

# 3mm × 3mm Monolithic DC/DC Boost/Inverting Converters with 65V Power Switches

**Joshua Moore**

The vast array of power supply rails required by modern electronics has popularized the use of compact, easy-to-use monolithic DC/DC converters, such as the LT3580 boost/inverting converter. The LT8580, LT8570, and LT8570-1 build on the success of the LT3580, increasing the switch voltage to 65V and the input voltage to 40V, while retaining features and pin compatibility. The LT8580 includes a 65V, 1A power switch, whereas the LT8570 and LT8570-1 step the switch current limit down to 0.5A and 0.25A, respectively. Various current options enable application optimization—a monolithic converter sized for specific demands can be smaller and more efficient than one designed for greater load currents. Optimized sizing for current limit helps limit input and output current in the event of a short or failure.

In addition to the new options, all devices in the family—LT®3580, LT8580, LT8570, and LT8570-1—are pin compatible. With a few simple component changes, the same PCB layout can be used for a range of applications, allowing fast turnaround design changes and reuse. The LT8580, LT8570, and LT8570-1 retain the LT3580's features such as single resistor feedback, for both positive and negative output voltages, overtemperature protection, frequency foldback, and an external clock input pin. And, like the LT3580, many features are user adjustable, including oscillator frequency, soft-start, UVLO and output voltage. All are available in thermally enhanced 8-pin 3mm × 3mm DFN or 8-pin MSE packages.

## 65V POWER SWITCH

The LT8580/LT8570/LT8570-1 incorporate an internal 65V power switch, for applications with high input and output voltages. Furthermore, $V_{IN}$ is capable of handling up to 40V. This can greatly simplify applications. For example, Figure 1 shows the necessary circuitry to create a 48V output with the LT3580; the LT8570's 65V switch simplifies the circuit in Figure 2.

**Table 1. Feature comparison of monolithic pin-compatible boost/inverting DC/DC converters**

| | LT3580 | LT8570 | LT8570-1 | LT8580 |
|---|---|---|---|---|
| Input Range | 2.5V to 32V | 2.55V to 40V | 2.55V to 40V | 2.55V to 40V |
| Max Switch Voltage | 42V | 65V | 65V | 65V |
| Max Switch Current | 2A | 1A | 0.5A | 0.25A |
| Integrated Power Switch | ✓ | ✓ | ✓ | ✓ |
| Frequency Foldback | ✓ | ✓ | ✓ | ✓ |
| External Clock Input | ✓ | ✓ | ✓ | ✓ |
| Overtemperature Protection | ✓ | ✓ | ✓ | ✓ |
| Positive And Negative Output Voltages | ✓ | ✓ | ✓ | ✓ |
| Single Resistor Feedback | ✓ | ✓ | ✓ | ✓ |
| Packages | 8-Pin MSE | 8-Pin MSE | 8-Pin MSE | 8-Pin MSE |

All devices in the family—LT3580, LT8580, LT8570, and LT8570-1—are pin compatible. With a few simple component changes, the same PCB layout can be used for a wide variety of applications, allowing fast turnaround design changes and reuse.

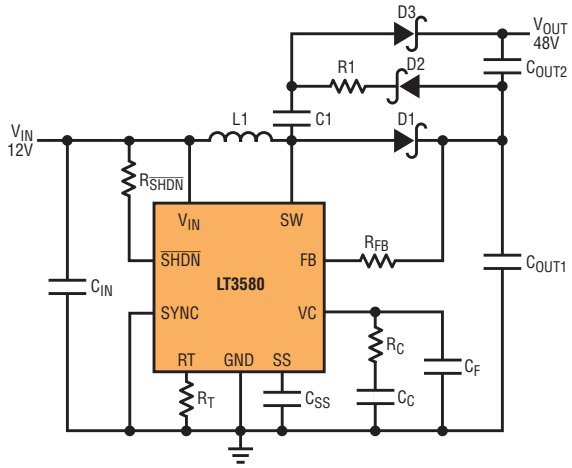


Figure 1. LT3580 configured for 48V output

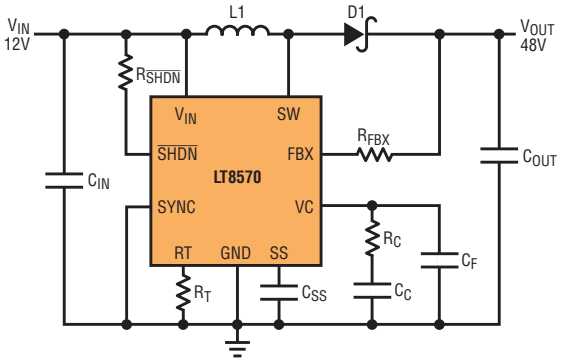


Figure 2. LT8570 configured for 48V output

## USER CONFIGURABILITY

The LT8580, LT8570 and LT8570-1 include a number of configuration options. The oscillator frequency can be adjusted from 200kHz to 1.5MHz. While lower switching frequencies tend to be more efficient, higher switching frequencies offer smaller solution sizes. Also, choice of oscillator frequency may be useful for avoiding interference with sensitive RF circuitry.

Another configuration option is undervoltage lockout, which, for most applications, is configurable with just one resistor from $V_{IN}$ to $\overline{SHDN}$. This allows the parts to be used in situations where source impedance may be high, the source may ramp slowly or where it is desirable that the part not discharge the source below some threshold.

A final configuration option is soft-start. By varying the soft-start capacitor, the user can adjust the rate of increase of the inductor current. The faster the inductor current increases, the faster the output rises during start-up. However, allowing the inductor current to increase slowly reduces output voltage overshoot and avoids large input transient currents during start-up.

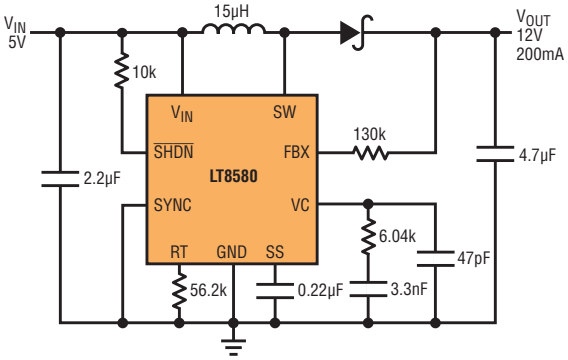


Figure 3. LT8580 configured as 5V input to 12V output boost converter

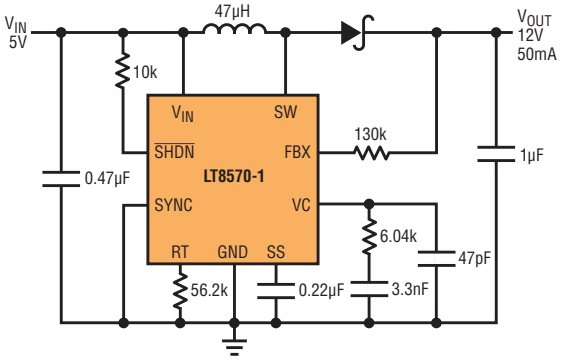


Figure 4. LT8570-1 configured as a 5V input to 12V output boost converter

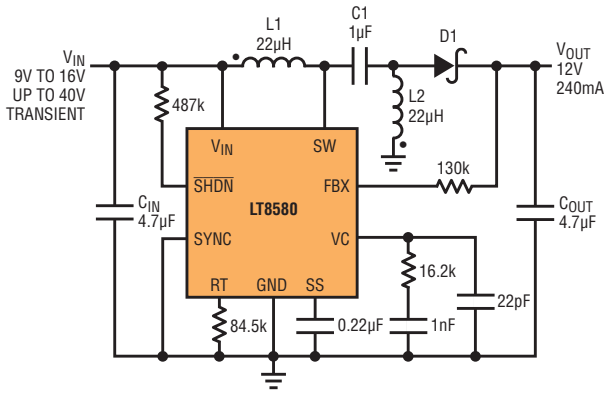


Figure 5. LT8580 configured as 9V–16V In to 12V output SEPIC converter

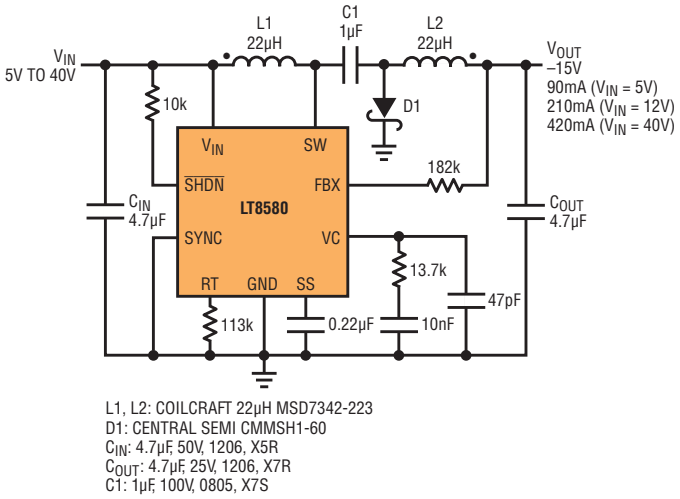


Figure 6. LT8580 configured as 5V–40V In to –15V out dual inductor inverting converter

## SIMPLE AND EASY OUTPUT VOLTAGE CONFIGURATION

The FBX pin on LT8580/LT8570/LT8570-1 makes setting output voltage easy for both inverting and noninverting topologies. In both cases, only a single resistor from $V_{OUT}$ to FBX is needed to set the output voltage—the converter topology determines whether the output is positive or negative.

## BOOST CONVERTER

The boost topology creates an output voltage greater than the input voltage. Since the boost converter is the simplest topology for LT8580, LT8570, and LT8570-1, it can clearly illustrate how the different current limits affect solution size. Figure 3 shows the LT8580 in a 12V out boost converter and Figure 4 shows the LT8570-1 in the same converter. Note that the only significant circuit changes required between the two are the inductor, the input capacitor, and the output capacitor. Both applications use similar inductors in the Würth WE-LQS family, but the LT8580 requires an inductor that is 5mm × 5mm, while LT8570-1 can use an inductor that is only 3mm × 3mm. This reduces the inductor footprint from 25mm² to 9mm². At the same time, the height drops from 4mm to 1.5mm. Also, where LT8580 required 0805 size capacitors, the LT8570-1 can use 0603 size capacitors.

## SEPIC CONVERTERS

The SEPIC topology creates a positive voltage where the input voltage may be less than or greater than the output voltage. Due to a lack of DC path from input to output, it also offers output disconnect, so that there is no output voltage if the converter is shut down. Output disconnect makes the converter resistant to damage in case of output shorts. The application in Figure 5 shows the LT8580 configured to produce 12V from an input range of 9V to 16V, and able to survive 40V transients on $V_{IN}$.

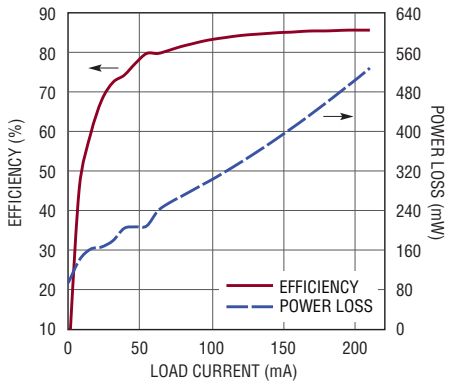


Figure 7. Efficiency and power loss for Figure 6 with $V_{IN}$ = 12V

## DUAL INDUCTOR INVERTING CONVERTER

The dual inductor inverting topology creates a negative voltage from a positive input voltage, which may be greater than or less than the magnitude of the output voltage. This topology, like the SEPIC, has output disconnect. In addition, this topology tends to have a quieter output than the boost or SEPIC, since L2 is in series with the output. The converter in Figure 6 shows the LT8580 configured as a dual inductor inverting converter with a –15V output, and Figure 7 shows the efficiency and power loss versus load.

## CONCLUSION

The popular LT3580 monolithic boost/inverting converter has been joined by the pin-compatible LT8580, LT8570, and LT8570-1 converters, which add current options and higher voltages, while retaining the features of the LT3580. These new options provide an additional means of optimizing a power supply for a given application. Depending on the intended load, solution size and part counts can be reduced. By retaining pin compatibility, transition within the LT3580, LT8580, LT8570 and LT8570-1 family of parts is easy, allowing simple design changes and PCB reuse. ■

# One LED Driver Is All You Need for Automotive LED Headlight Clusters

**Keith Szolusha and Kyle Lawrence**

Low beam headlights, high beam headlights, daytime running lights and signal lights are often fashioned together in a single unit or cluster, allowing designers to produce distinctive automotive front end looks. LED lighting has found its way into these clusters, distinguishing the high end faces of today's luxury vehicles; but LEDs offer more than just good looks. They have a number of technical advantages over competing lighting technologies—notably improved efficiency, robustness and lifetime. Despite these advantages, automobile lighting designers are challenged by the cost of replacing traditional lamps with LEDs.

A significant portion of the cost LED lighting is driven by the costs of the LEDs themselves, thermal management assemblies (such as finned metal heat sinks) and robust LED driver circuits. Traditionally, each LED beam or light type would require its own LED driver PCB. Costs and complexity can be significantly reduced if a single driver is used to drive multiple LED strings (in series) within the lighting cluster.

A comprehensive, multi-LED-string driver must support the high voltages and high currents required by high power LED strings. It must also deftly handle the on/off transitions of some LED strings while others remain on and unaffected. In an automotive environment, it should accommodate wide ranging input and output voltages, of the battery at the input and the LED strings at its output. Automotive environments also demand that the driver feature low EMI and open and short-circuit fault protection.

The LT3795 and LT3952 automotive LED drivers satisfy these requirements when used in boost and (patent-pending) boost-buck topologies. These LED drivers can operate in high voltage boost (step-up)

Figure 1. LT3795 70W (70V 1A) automotive boost LED driver drives daytime running lights, low beam, and high beam strings in series with 95% efficiency.

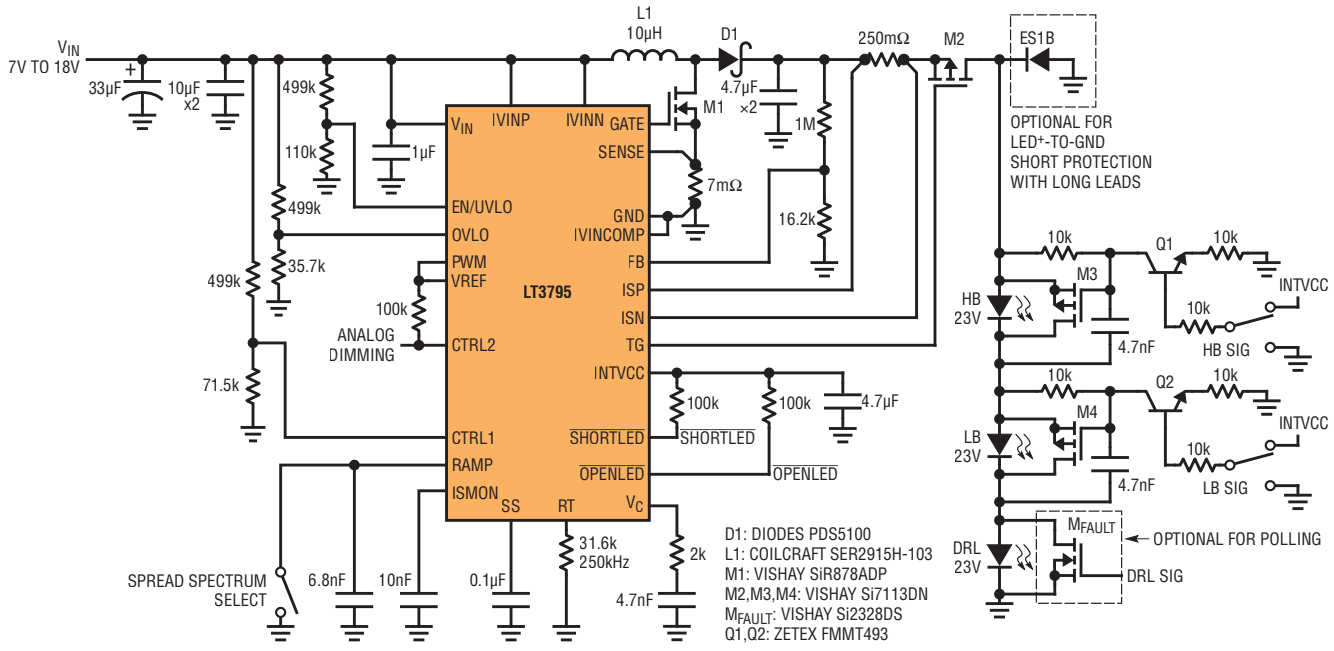

The LT3795 and LT3952 automotive LED drivers can operate in high voltage boost (step-up) and boost-buck (step-up and step-down) topologies—driving series-stacked LED strings directly from a wide automotive battery voltage range.

and boost-buck (step-up and step-down) topologies. They support large stacks of LED strings, accept a wide battery voltage range and can gracefully transition the number of ON LEDs in the output. They both feature spread spectrum frequency modulation for reduced EMI and short and open LED protection.

## BOOST LED DRIVER FOR LOW BEAM, HIGH BEAM, AND DAYTIME RUNNING LIGHT

The total voltage of a low beam, high beam and daytime running light headlight cluster can be about 70V when driven with 1A LEDs. The 100V+ LT3795 single channel LED driver can drive 70W of LEDs directly from a standard 9V–16V automotive input—all three lights in the cluster can be driven in series.

The combination driver circuit in Figure 1 shows how the LT3795 single channel LED driver can be used to power 1A through the daytime running light, low beam and high beam headlights in a boost topology. This allows the low and high beam lights to be turned on and off—daytime running lights are always on.

As the low and high beams are turned on and off, their LED strings are added to and subtracted from the daytime running light strings by high current MOSFET switches M3 and M4. These switches act as shorting-out devices. When the MOSFET is on, it shorts out its corresponding beam, turning it off; when the MOSFET is off, the beam runs with 1A current. This easy-to-implement design is robust and saves significant space, requiring no extra controllers.

Switching an entire 23V beam string of LEDs (such as low beam) on and off creates a 23V transient on the output. It is important that on and off transitions are not instantaneous. In this design, Q1 and Q2 control the MOSFET on and off transitions to prevent large spikes of LED string current, which would otherwise result as energy that is taken up or released by the output cap. Instantaneously switching M3 and M4 would drop the LED current temporarily to zero, causing a visible blink in the low beam lights, or it could induce a high current spike, up to 3A, that would stress even the most robust LED string.

Figure 2 shows the controlled switching of M3 and M4, transitioning the LED current and output voltage over ~500µs. The shorting-out driver for M3 and M4 works at a rate at which the output capacitor and the converter can handle slow transients with less than 20% deviation in output current over a very short

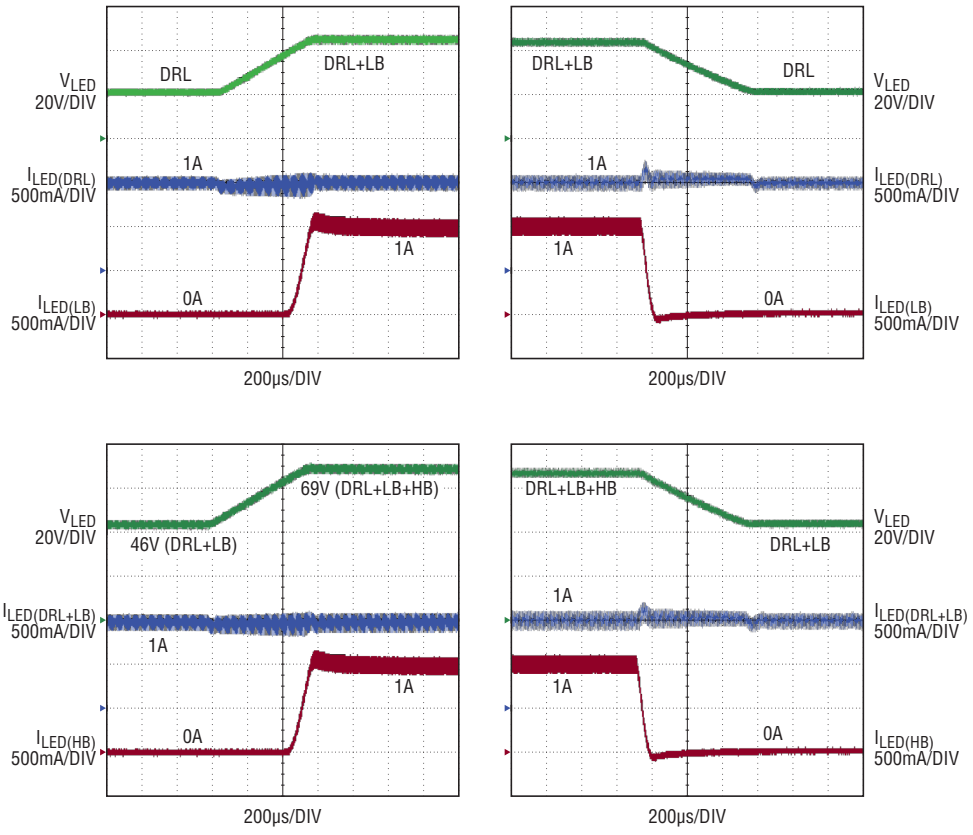


**Figure 2. All cluster LED strings are driven in series by one IC channel, but no running string is significantly affected by turning on (or off) other strings—constant brightness is maintained even as low beam and high beam strings are turned on and off. Transitions are controlled by slowly switching on or off LED beams with shorting-out MOSFETs, preventing current spikes on other, unchanged strings.**

In the combination driver circuit, the LT3795 single channel LED driver can be used to power 1A through the daytime running light, low beam and high beam headlights in a boost topology. This allows the low and high beam lights to be turned on and off—daytime running lights are always on.

time. There is no perceivable blinking or flicker in the low beam or other running lights when a string is added to or subtracted from the always-on running lights.

The LT3795 boost LED driver circuit in Figure 1 has 91% and 95% efficiency when only daytime running lights are on, and when all beams are on, respectively. It has short-circuit and open LED protection. With good layout and sufficient copper area for the discrete power components, the highest temperature rise component of this 70W boost driver can be kept under 40°C without additional heat sinks or airflow. EMI filters, a GATE drive resistor and spread spectrum frequency modulation can be used for reduced EMI.

## BOOST-BUCK LED DRIVER FOR DAYTIME RUNNING LIGHT AND SIGNAL LIGHT COMBO

Some vehicles use LED lighting for daytime running lights and signal lights, but not for high or low beams. Daytime running lights are designed in a variety of different configurations, from long strings of LEDs with relatively low current to short strings with high current. An IC that can support both step-up and step-down conversion can power a combination daytime running light and sometimes-on trim light or amber signal light. Using an IC that can seamlessly handle transitions of stacked-string voltages in a step-up and step-down topology allows designers to focus on light aesthetics and functionality, without

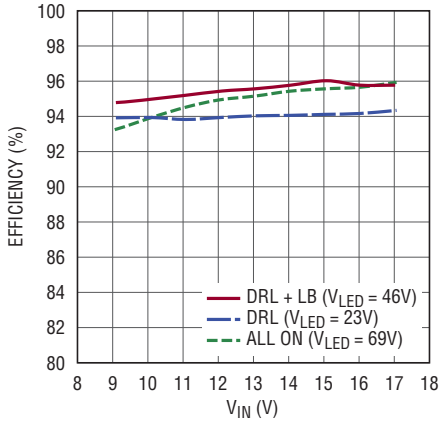


Figure 3. Efficiencies of various light combinations are between 94% and 96%.

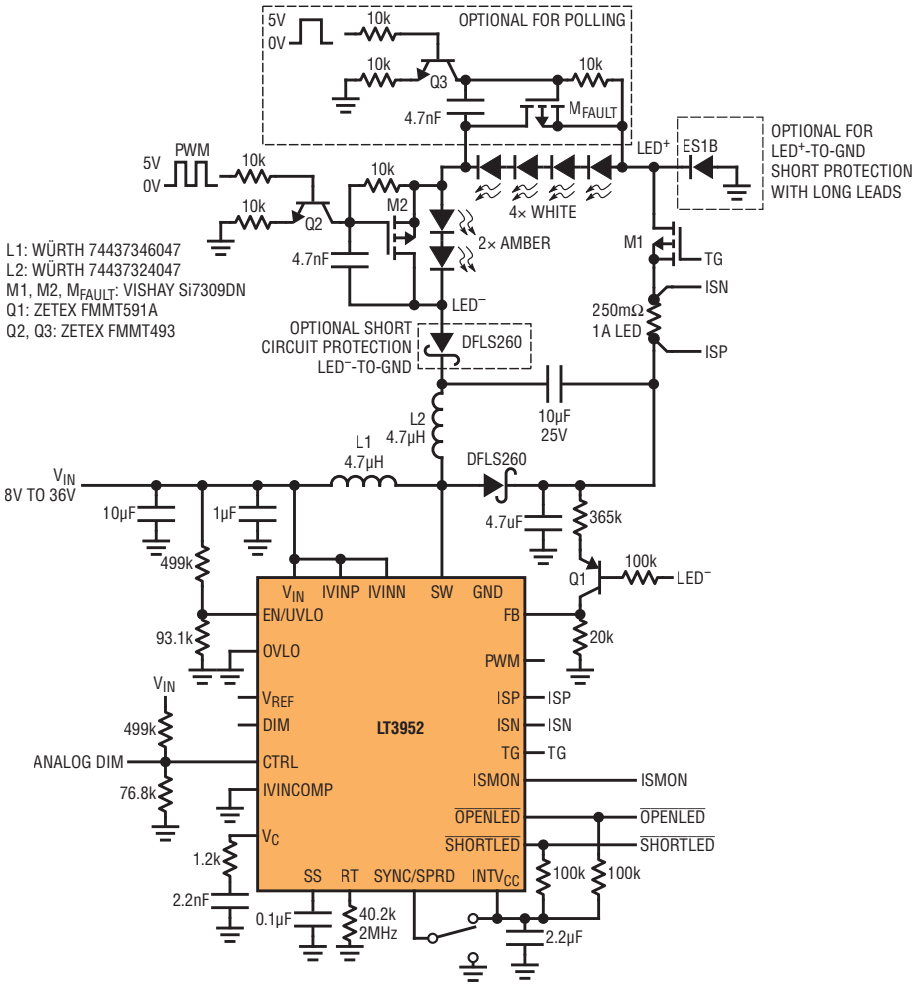


Figure 4. This 18W (18V, 1A) automotive boost-buck LED driver runs daytime running lights and amber signal lights at different brightness levels. 2MHz switching frequency keeps EMI above and outside the AM band.

In automotive environments, it is important that a failure of one lamp function not impede operation of other LEDs. The LT3795 and LT3952 include fault detection and reporting features that enable a system controller to turn on operational LEDs, even when other strings in the series are faulty.

worrying about the driver. Dimming can be thrown into the mix with little effort.

The (patent-pending) boost-buck LT3952 LED driver in Figure 4 regulates 1A through a compact daytime running light and a series amber signal or trim light. The 2-LED amber light can be blinked or PWM-dimmed via the M2 shorting-out MOSFET without affecting the brightness of the constantly running daytime running light.

The result is a single, compact 1A boost-buck LED driver whose output drives a visibly steady daytime running light of 2–4 LEDs, and a blinking signal light and/or variably dimmed trim light.

LED current transients are minimized by the controlled switching of MOSFET M2—which turns on to short out the amber light and turns off to enable the amber light. Figure 5 shows PWM dimming of the amber light operates at 120Hz for flicker-free 10:1 dimming without affecting the brightness of the daytime running light. Similarly, it can be blinked on and off at 1Hz—say 10%-dimmed "off" (or other) to 100% "on" to act as a turn signal light.

The new boost-buck LED driver topology allows the input voltage and output voltage ranges to cross over each other, simplifying design by reducing the need for pre-regulation.

**Figure 5. PWM dimming amber signal lights at 10:1 (and up to 20:1) at 120Hz does not affect the LED string current of the daytime running lights.**

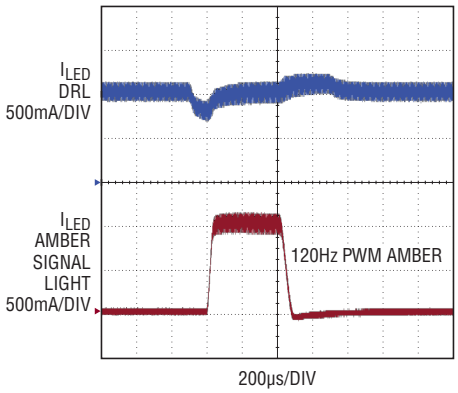


**Figure 6. Similar automotive boost-buck LED driver to Figure 4, but this one uses a switching frequency of 350kHz for improved efficiency.**

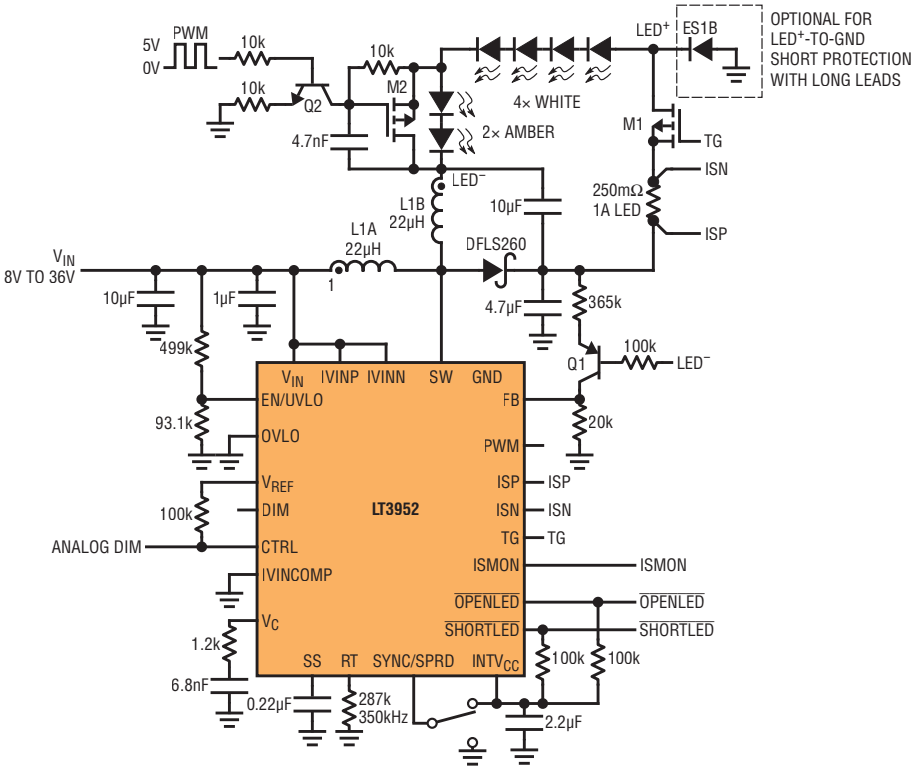

The converter is short-circuit and open LED protected. An optional low $V_F$ diode in the LED⁻ path provides LED⁻-to-GND protection in addition to the LED⁺-to-GND protection from the TG MOSFET (M1) and LT3952 overcurrent detection. The boost-buck topology has both low input and low output ripple for very low EMI, which is reduced even further with spread spectrum frequency modulation.

The converter is short-circuit and open LED protected. An optional low $V_F$ diode in the LED⁻ path provides LED⁻-to-GND protection in addition to the LED⁺-to-GND protection from the TG MOSFET (M1) and LT3952 overcurrent detection. The boost-buck topology has both low input and low output ripple for very low EMI, which is reduced even further with spread spectrum frequency modulation.

To improve efficiency, the converter can be operated at a switching frequency of 350kHz (Figure 6). Efficiencies of the two options are compared in Figure 7. Note that the 2MHz solution has the advantages of a reduced size inductor, and EMI above and outside of the AM band. At either 350kHz or 2MHz, uncoupled inductors can be used in place of the single, coupled inductor in the boost-buck topology.

**Figure 7. Comparison of efficiency of 350kHz boost-buck solution (Figure 6) and 2MHz solution (Figure 4).**

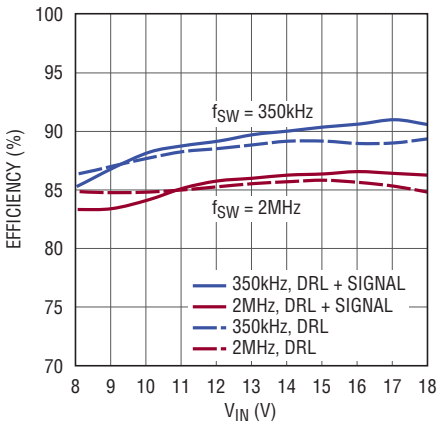


## SHORT AND OPEN POLLING

In automotive environments, it is important that a failure of one lamp function does not impede operation of other LEDs. The LT3795 and LT3952 include fault detection and reporting features that enable a system controller to turn on operational LEDs, even when other strings in the series are faulty.

Using the fault flags and an additional, optional diagnostic switch ($M_{FAULT}$), the system computer can poll the LED beams by turning them on and off to determine which one has an open. The system controller can run the remaining non-faulty LED beams while the faulty beam is shorted out. The faulty string can be re-polled, and brought online as soon as it is healthy again. Both the LT3795 and LT3952 circuits handle short and open circuits, so shorting and opening strings poses no potential harm for the circuits.

Additional voltage readings and short-circuit detections can be put in place to turn off strings that have been shorted, or to report shorted segments that require servicing. The LED driver circuits maintain functionality and reliability even when one of the LED strings has been damaged.

## CONCLUSION

Combination automotive LED lights can be driven from a single-channel LED driver to save cost and space. High power and high voltage strings can be stacked in a boost topology, or various brightness or lower voltage strings can be turned on and off in the new, boost-buck topology. Using a single driver for several strings saves cost and complexity while retaining aesthetic benefits.

The LT3795 and LT3952 are powerful and flexible LED driver ICs that can be used for combination headlight cluster LED strings. They feature high voltage, high current, spread spectrum frequency modulation, and short-circuit and open LED protection. ■

# What's New with LTspice IV?

**Gabino Alonso**

twitter—Follow @LTspice at *www.twitter.com/LTspice*
—Like us at *facebook.com/LTspice*

### BLOG BY ENGINEERS, FOR ENGINEERS

Check out the LTspice® blog (www.linear.com/solutions/LTspice) for tech news, insider tips and interesting points of view.

**New Article: "Parallel MOSFETs in Hot Swap Circuits" by Dan Eddleman**
**www.linear.com/solutions/5677**

While it is often desirable, and sometimes absolutely critical, to use multiple parallel MOSFETs in Hot Swap™ circuits, careful analysis of safe operating area (SOA) is essential. Each additional parallel MOSFET added to a circuit improves the voltage drop, power loss, and accompanying temperature rise of the application. But, the parallel MOSFETs do not necessarily improve the transient power capability of the circuit. Unless every MOSFET is driven by an independent control loop, temporary high power events such as initial turn-on into a load or current limiting into a short-circuit fault have a tendency to concentrate the power into a single MOSFET. That being said, it is safe to connect MOSFETs in parallel to reduce the overall resistance, using a single control loop as long as each MOSFET's SOA is capable of withstanding the entire transient event.

## What is LTspice IV?

LTspice® IV is a high performance SPICE simulator, schematic capture and waveform viewer designed to speed the process of power supply design. LTspice IV adds enhancements and models to SPICE, significantly reducing simulation time compared to typical SPICE simulators, allowing one to view waveforms for most switching regulators in minutes compared to hours for other SPICE simulators.

LTspice IV is available free from Linear Technology at www.linear.com/LTspice. Included in the download is a complete working version of LTspice IV, macro models for Linear Technology's power products, over 200 op amp models, as well as models for resistors, transistors and MOSFETs.

### SELECTED DEMO CIRCUITS

For a complete list of example simulations utilizing Linear devices, please visit www.linear.com/democircuits.

#### Linear Regulators

- **LT3086:** Adjustable voltage controlled current source www.linear.com/solutions/4475

#### Buck Regulators

- **LT8610AC:** 5V, 3.5A, 2MHz step-down converter (5.5V–42V to 5V at 3.5A) www.linear.com/solutions/5721
- **LTC3892:** High efficiency dual 3.3V/36V output step-down converter (7.5V–60V to 3.3V at 5.0A & 36V at 2A) www.linear.com/solutions/5668
- **LTM®4623:** Ultrathin 3A buck µModule® regulator (4V–20V to 1.5V at 3A) www.linear.com/solutions/5520

#### Boost Regulators

- **LT8580:** 1.5MHz, 5V to 12V boost converter (3.5V–6V to 12V at 200mA) www.linear.com/solutions/5236

#### Buck-Boost Regulators

- **LTC3111:** 15V, 800kHz wide input voltage buck-boost regulator (2.5V–15V to 5V at 1.5A) www.linear.com/solutions/4714
- **LTC3114-1:** Wide $V_{IN}$ range regulator with bootstrapped LDO (2.7V–40V to 5V at 1A) www.linear.com/solutions/5084

#### SEPIC Converters

- **LT8495:** 450kHz, 5V output SEPIC converter (3V–60V to 5V at 1A) www.linear.com/solutions/5727

#### Multitopology Converters

- **LT8471:** Dual output buck & inverting converter (6V–32V to +5V at 1.4A & –5V at 800mA) www.linear.com/solutions/4676

#### Isolated Converters

- **LT3798/LT8309:** Energy Star compliant isolated converter (85V–150VAC to 5V at 2.2A) www.linear.com/solutions/5623

#### Surge Stoppers

- **LTC3810:** High efficiency switching surge stopper (36V–75V to 57Vclamp at 5A) www.linear.com/solutions/5639

#### Hot Swap Design

- **LTC4218:** 12V/100A Hot Swap design using parallel MOSFETs www.linear.com/solutions/5685

#### Filter Building Blocks

- **LT1568:** Multiple examples of bandpass, lowpass and highpass filters, and a sine wave converter www.linear.com/solutions/5740

### SELECT MODELS

To search the LTspice library for a particular device model, choose Component from the Edit menu or press F2. Since LTspice is often updated with new features and models, it is good practice to

update to the current version by choosing Sync Release from the Tools menu. The changelog.txt file (see root installation directory) list provides a revision history of changes made to the program.

### Buck Regulators

- **LTC3882:** Dual output PolyPhase® step-down DC/DC voltage mode controller with digital power system management www.linear.com/LTC3882

### LED Drivers

- **LT3952:** 60V LED driver with 4A switch current www.linear.com/LT3952

### Supercapcitor Chargers

- **LTC3128:** 3A monolithic buck-boost supercapacitor charger and balancer with accurate input current limit www.linear.com/LTC3128

### Hot Swap Controllers

- **LTC4232-1:** 5A integrated Hot Swap controller (PCIe compliant) www.linear.com/LTC4232-1
- **LTC4234:** 20A guaranteed SOA Hot Swap controller www.linear.com/LTC4234

### Op Amps

- **LTC6268-10/LTC6269-10:** Single/dual 500MHz ultralow bias current FET input op amp www.linear.com/LTC6268 ■

## Power User Tip

### SIMPLE IDEALIZED DIODE

LTspice semiconductor diode models are essential for simulations, especially when you want to see results that include breakdown behavior and recombination current. However, as complete as the semiconductor diode model is in LTspice, there are times when you need a simple "idealized diode" model to quickly simulate, for example, an active load, a current source or a current limiting diode. To assist, LTspice provides a representation of an idealized diode model.

To use of this idealized model in LTspice, insert a .model statement for a diode (D) with a unique name and define one or more of the following parameters: Ron, Roff, Vfwd, Vrev or Rrev.

```
.model MyIdealDiode D(Ron=1 Roff=1Meg Vfwd=1 Vrev=2)
```

The idealized diode model in LTspice has three linear regions of conduction: on, off and reverse breakdown. The forward conduction and reverse breakdown can further be specified with current limit parameters Ilimit and revIlimit.

```
.model MyIdealDiode D(Ron=1 Roff=1Meg Vfwd=1
  Vrev=2 Ilimit=1 RevIlimit=1)
```

Furthermore, to smooth the switch between the off and conducting states the parameters epsilon and revepsilon can also be defined.

```
.model MyIdealDiode D(Ron=1 Roff=1Meg Vfwd=1 Vrev=2
  Ilimit=1 RevIlimit=1 Epsilon=1 RevEpsilon=1)
```

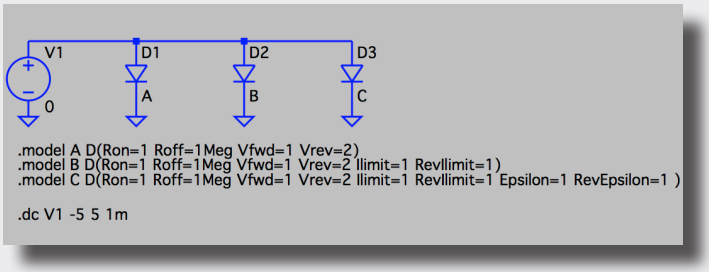


A quadratic function is also used between the off and on state such that the idealized diode IV curve is continuous in value and slope, so that the transition occurs over a voltage specified by the value of epsilon and revepsilon.

Once you have inserted your .model statement in your schematic you can edit the diode symbol's Value in the component attributes (Ctrl + Right Click) to match the name you specified in your statement. For more information on LTspice diode models, please refer to the help topics (F1).

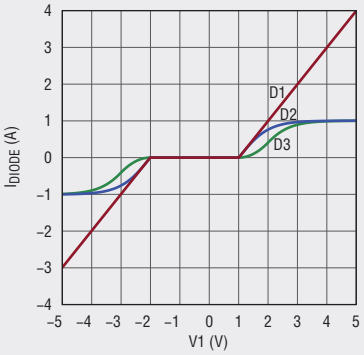


Just for fun, in the circuit example below an idealized diode model is used to simulate a MOSFET's $R_{DS(ON)}$ in an otherwise nonsynchronous step-down controller. By using an idealized diode model instead of the traditional Schottky diode, the conduction losses of synchronous rectification can be easily compared.

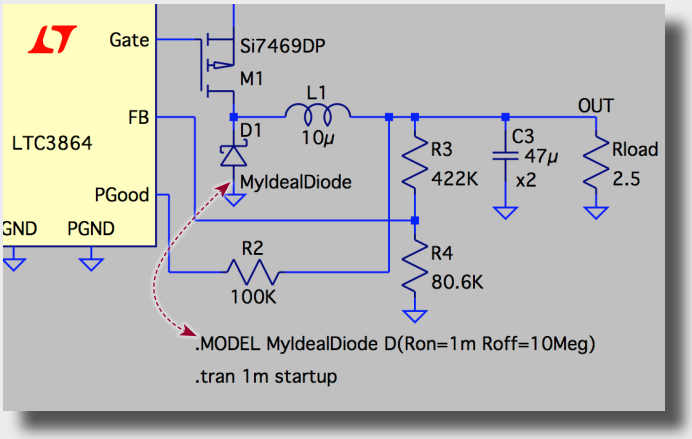


*Happy simulations!*

# Extend Remote Sensor Battery Life with Thermal Energy Harvesting

**Dave Salerno**

Wireless and wired sensor systems are often found in environments rife with ambient energy, ideal for powering the sensors themselves. For instance, energy harvesting can significantly extend the lifetime of installed batteries, especially when power requirements are low, reducing long-term maintenance costs and down time. In spite of these benefits, a number of adoption roadblocks persist. The most significant is that ambient energy sources are often intermittent, or insufficient to power the sensor system continuously, where primary battery power sources are extremely reliable over the course of their rated life. System designers may be reluctant to upgrade systems to harvest ambient energy, especially when seamless integration is paramount. The LTC3107 aims to change their minds by making it easy to seamlessly extend battery life, by adding energy harvesting to existing designs.

With the LTC3107, a point-of-load energy harvester requires little space, just enough room for the LTC3107's 3mm × 3mm DFN package and a few external components. By generating an output voltage that tracks that of the existing primary battery, the LTC3107 can be seamlessly adopted to bring the cost-savings of free thermal energy harvesting to new and existing battery-powered designs.

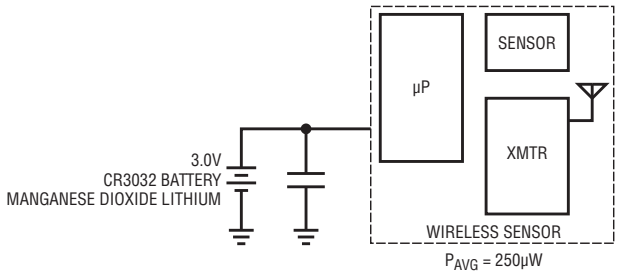


**Figure 1. Simplified diagram of a typical battery-powered wireless sensor system**

The LTC3107, along with a small source of thermal energy, can extend battery life, in some cases up to the shelf life of the battery, thereby reducing the recurring maintenance costs associated with battery replacement. The LTC3107 is designed to augment the battery, or even supply the load entirely, depending on the load conditions and harvested energy available.

A digital output, BAT_OFF, is provided to indicate whether or not the battery is being used to power the load at any given time. This allows the system to monitor the effectiveness of the harvester, and the duty cycle of the battery's usage for maintenance reporting. BAT_OFF is internally pulled up to $V_{OUT}$.

Figure 1 shows a typical wireless sensor application. This system is powered entirely by a CR3032 3.0V primary lithium coin cell with a capacity of 500mA-Hr. The battery will last about eight months in continuous operation if the average system power demand is 250µW.

Figure 2 shows the same system, using the same battery, with the addition of the LTC3107-based thermal harvester to extend the battery life.

Figure 3 shows the predicted battery life extension with the addition of thermal energy harvesting, using a small (15mm × 15mm) thermoelectric generator (TEG) and a 24mm² heat sink over a range of TEG mounting surface temperatures (assuming a 23°C ambient).

In situations where the harvested thermal power is greater than the average power required by the load, the battery is never used to power the load—only 80nA of current is drawn from the battery—resulting in a battery life approaching the five to ten year shelf life of a typical primary battery. Under these conditions, the battery is used only as a reference voltage for the LTC3107 to provide the output voltage regulation target. It is important to note that the

The LTC3107, along with a small source of thermal energy, can extend battery life, in some cases up to the shelf life of the battery, thereby reducing the recurring maintenance costs associated with battery replacement.

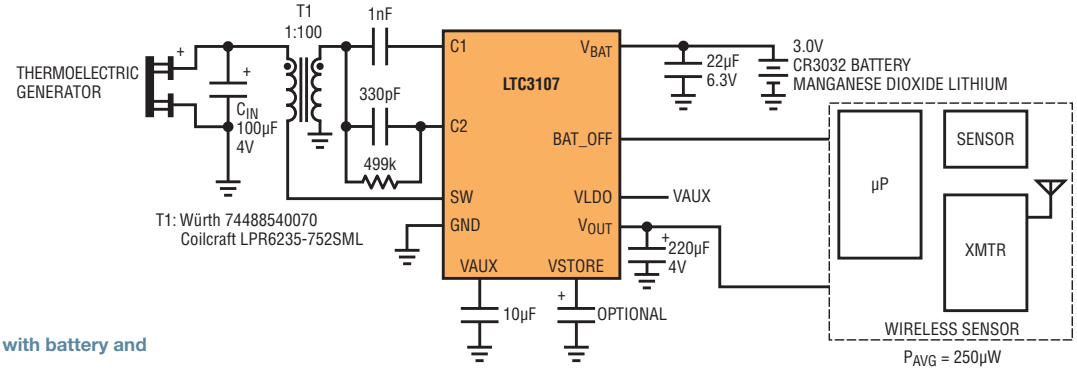


**Figure 2. Wireless sensor system with battery and the LTC3107 thermal harvester**

LTC3107 prevents any charge current into the battery under all operating conditions.

For example, for the system shown in Figure 2, with the TEG attached to a harvesting heat source, such as a warm pipe or piece of machinery just 12°C above ambient temperature, the LTC3107 can power the 250µW load entirely with harvested energy, resulting in the elimination of many battery service replacements over the shelf life of the battery, as shown in Figure 3.

The waveforms of Figure 4 show the battery voltage and the LTC3107 output voltage. As shown, the output voltage is regulated about 30mV below the unloaded battery voltage—seamless and transparent to the system load—providing an output voltage for which the system is designed. Under these conditions, the BAT_OFF output remains high, indicating that the battery is not being used to power the load. (Note that in these figures, the resistive loading of the scope probe has lowered the BAT_OFF high voltage below $V_{OUT}$ due to the resistor divider formed by the probe and the pull-up resistor internal to the LTC3107.)

If the load demand exceeds the harvester's capability, the battery is used as needed to maintain the output voltage and provide the necessary output power required by the load. In these cases, the harvester supplies as much of the load current as possible to minimize current from the battery, and maximize battery life. The BAT_OFF signal remains low, even though some of the load current is supplied by the harvester. The waveforms for this condition are shown in Figure 5. Note that under these conditions, $V_{OUT}$ is regulated by the LTC3107 to about 220mV below the actual battery voltage.

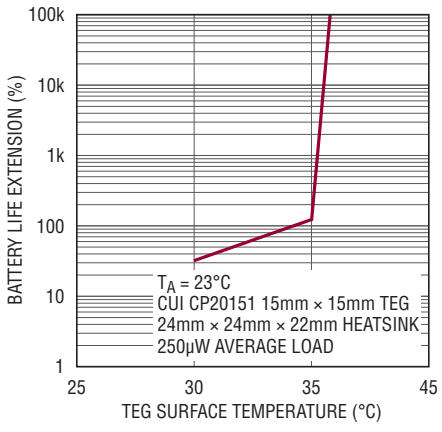


**Figure 3. Battery life can be extended by years by using a thermal harvester**

If the load is dynamic, transitioning from low to high values, then the BAT_OFF signal may be pulsing high and low, indicating when the harvester is able to supply the load and when the battery is needed. This is illustrated in the waveforms of Figure 6, which occurred during a momentary load step.

To further extend battery life, the LTC3107 can store excess harvested energy in a large-valued capacitor on the VSTORE pin during light load conditions to support $V_{OUT}$ during periods of heavy load. To facilitate the use of supercapacitors, which typically have a maximum voltage rating of 5V, the voltage on VSTORE is internally clamped to 4.48V maximum.

This energy storage feature reduces or eliminates battery drain during times of increased load by automatically using stored energy to maintain $V_{OUT}$ before

resorting to battery power. This is illustrated in the waveforms of Figure 7. Here, the VSTORE voltage, having charged up during a period of light load, can be seen dropping during a period of increased load as it delivers energy to the load. It can be seen that $V_{OUT}$ does not drop and the BAT_OFF signal remains high, indicating that the battery was not used to support the output, even during the load transient.

In situations where no harvested power is available and any stored energy is depleted, the output power is supplied entirely by the battery, just as it was without the harvester, and $V_{OUT}$ is regulated 220mV below the battery voltage. In this case, the harvester circuitry remains idle, adding only 6µA load to the battery. The harvester waveforms in this scenario would be the same as in Figure 5.

To protect the battery from short circuits on $V_{OUT}$, the current from VBATT to $V_{OUT}$ is limited to 30mA minimum and 100mA maximum. Therefore, steady-state loads of at least 30mA can be supported when running from the battery. If needed, higher transient loads can be supported for short durations with the help of the decoupling capacitor on $V_{OUT}$.

The steady-state output current produced by the harvester is dependent on several factors, but is primarily limited by the temperature differential that can be impressed across the TEG. Note that this is not only a function of the TEG mounting surface temperature and the ambient temperature, but by the thermal resistance of the heat sink used on the cool side of the TEG. The harvested output current can range from as little as microamps to several milliamps steady state. The current that can be supplied to $V_{OUT}$ from VSTORE is limited by the differential voltage between the two pins and the internal path resistance through the LTC3107 charge control circuitry, which is about 120Ω typical. Therefore the VSTORE current is typically limited to a few milliamps as well, and is not intended to support large load transients. These should be handled by the $V_{OUT}$ decoupling capacitor.

In addition to the BAT_OFF feature, the LTC3107 provides a second output voltage, regulated to 2.2V by an internal low dropout (LDO) regulator that can be used to power loads up to 10mA. The 2.2V LDO also gets its power from the harvester and the battery if necessary.

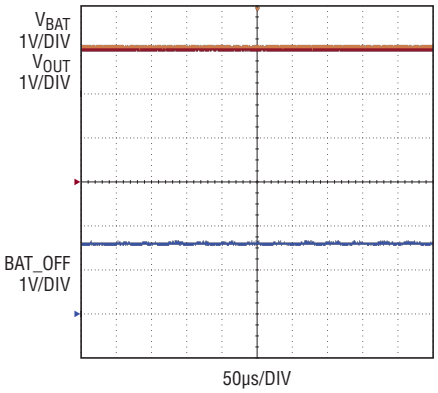


Figure 4. Harvester waveforms when $P_{HARVEST} > P_{LOAD}$

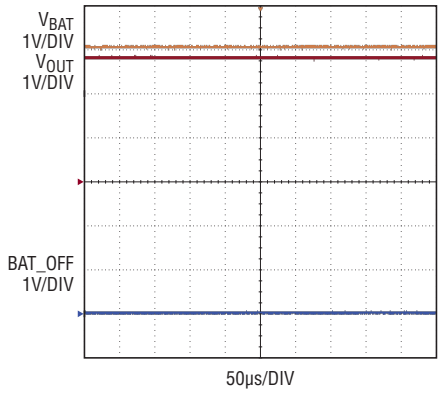


Figure 5. Harvester waveforms when $P_{HARVEST} < P_{LOAD}$

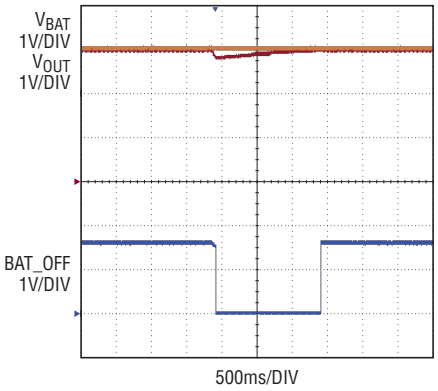


Figure 6. Harvester waveforms when a brief load transient exceeds $P_{HARVEST}$

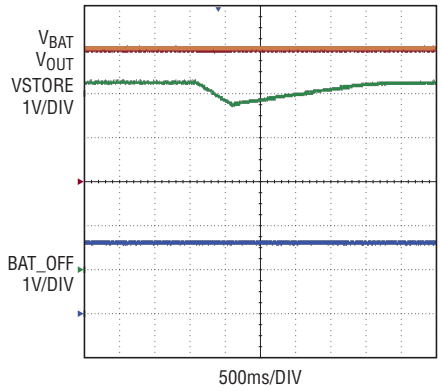


Figure 7. Using the VSTORE feature to support a momentary increase in load

## SUMMARY

To facilitate the adoption of thermal energy harvesting into a wide range of new and existing primary battery powered applications, the LTC3107 is designed to work with battery voltages in the range of 2V to 4V. This includes most of the popular long-life primary batteries used in lower power applications, such as 3V lithium coin cell batteries and 3.6V lithium-thionyl chloride batteries. The LTC3107 provides the best of both worlds—the reliability of battery power and the maintenance cost savings of thermal energy harvesting with minimal design effort. ■

# Simplify Small Solar Systems* with Hysteretic Controller

**Mitchell Lee**

Battery-based solar power systems in the 10W–100W range often use a switching regulator to control battery charge. These have the advantage of high efficiency and facilitate peak power point tracking, but only at the cost of an inductor, circuit complexity and noise. As a simpler alternative to a switching regulator, linear control is feasible in applications up to about 20W. While simple and quiet, linear charge controllers generate heat, which must be shed by means of a heat sink. The bulk, cost and assembly complexity of a heat sink somewhat nullify a linear charge controller's perceived advantages over a switching regulator approach.

A hysteretic controller that simply connects or disconnects the solar panel as needed to limit the battery's state of charge provides an excellent anodyne, one devoid of inductors, complexity, noise and heat sinking.

Both series and shunt hysteretic switch topologies are possible. A series configuration opens the connection to the solar panel when the battery has reached its maximum charging voltage, then reconnects when the battery voltage falls to a lower threshold. The chief difficulty with a series configuration is driving the high side switch, which requires either a charge pump for an n-channel implementation or a high voltage, high side gate drive circuit for a p-channel MOSFET.

The preferable shunt arrangement is shown in Figure 1. In this case the switch (S1) turns off when the battery voltage falls below a certain threshold, allowing the solar panel current to charge the battery. When the battery voltage exceeds a second, higher threshold, the switch turns on to divert solar panel current to ground. Diode D1 isolates the battery

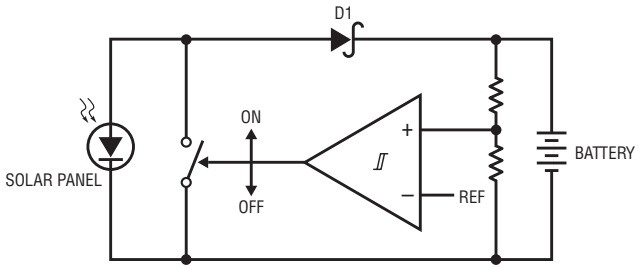


**Figure 1. Shunt mode hysteretic switch regulates battery charge in small solar system**

when S1 shorts the solar panel. The switch is easily implemented with an n-channel MOSFET, directly driven by the output of a ground-referred comparator.

Figure 2 shows a complete shunt charge controller for a 12V lead-acid battery using an LTC2965 100V micropower voltage monitor as the controlling element. While it is not monitoring 100V in this application, the LTC2965's 3.5V to 100V operating range generously encompasses the normal voltage range of a 12V battery, with plenty of margin.

The LTC2965 contains a ~78M, 10:1 divider which monitors the battery voltage at the $V_{IN}$ pin. Thresholds are generated from a precision 2.412V reference by a separate, external divider, and compared against the attenuated version of $V_{IN}$. This arrangement eliminates the need for precise, high value resistors in the main divider.

Hysteresis is developed by switching the comparator's inverting input back and forth between high and low thresholds as set at the INH and INL pins. These trip points determine the voltages at which battery charging commences and terminates.

Other important features include the LTC2965's low power operation (40µA total supply current including Q1's gate drive), built-in 0.5% accurate reference, and hysteretic operation with independent threshold adjustment.

Operation is as follows. Initially, with a battery voltage of less than 13.7V the comparator output is low and Q1 is off, allowing all available solar panel current

* Pun intended.

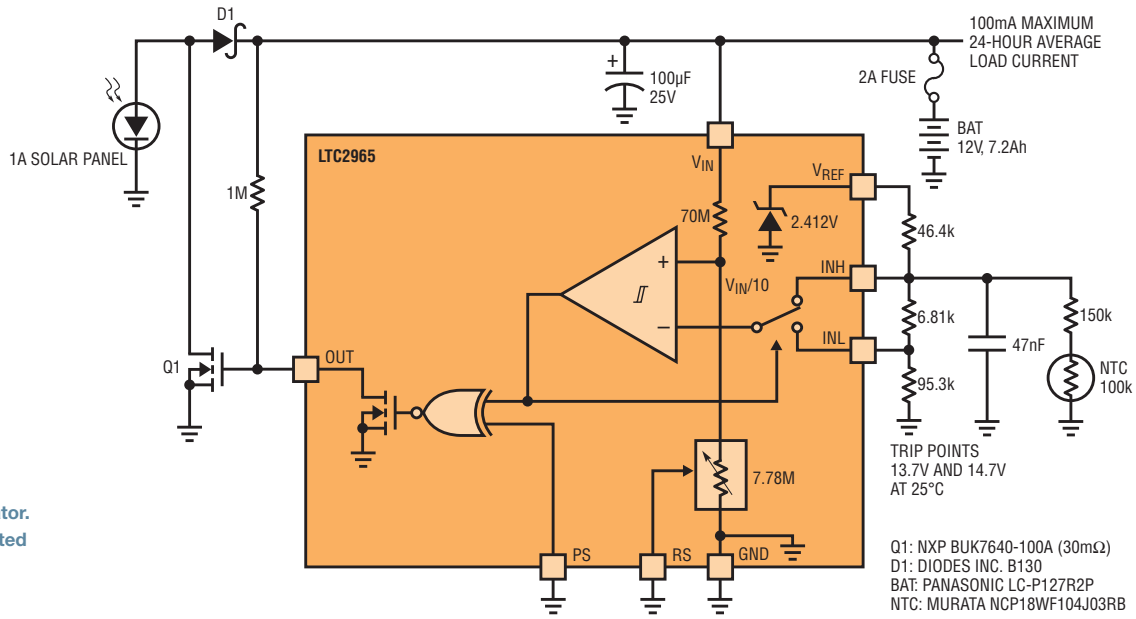


**Figure 2. Shunt mode hysteretic regulator. Trip points are temperature compensated from 0°C to 50°C**

to pass through D1 to the battery and load. As the battery charges, its voltage rises and upon reaching an upper charging limit of 14.7V, Q1 turns on, shorting the solar panel to ground. D1 isolates the battery from the shunt path. With Q1 on, the battery voltage falls at a rate dependent on the state of charge and the magnitude of the load current. When the battery voltage reaches a lower float limit of 13.7V, Q1 turns off and the panel current is, once again, applied to the battery and load.

This charging scheme shares certain attributes of cycle charging and trickle charging. Initial charging proceeds until the battery voltage reaches 14.7V, whereupon the circuit begins pulse charging to complete the process.

It is important to correctly size the battery and the solar panel for a specific application. As a general rule, choose a maximum or "peak" panel current equal to 10× the load current averaged over a 24-hour period, and a battery ampere-hour capacity equal to 100× this same averaged figure. Peak current of a 36-cell panel is estimated by dividing the panel's claimed "marketing" watts by 15. A 15W panel can be expected to produce ~1A maximum output current under favorable conditions, but this should be verified by actual measurement of the panel under consideration.

These relationships were derived for Milpitas, California to give 4 days' run time on unassisted battery power, with the panel oriented for maximum winter insolation. In the case of Figure 2, the circuit was designed for a continuous 100mA load (2.4Ah/day), dictating the use of a 1A panel and 10Ah battery. The somewhat smaller battery specified in Figure 2 is undersized for about 3 days' operating time, deprived of any solar input.

The charging thresholds are temperature compensated by an NTC thermistor over a 0°C to 50°C range. If operated in a controlled environment, temperature compensation is unnecessary and the thermistor and 150k resistor can be replaced by a fixed, 249k unit. For readers who wish to trim out errors introduced by the 1% resistors, Figure 3 shows a simple scheme for adjusting the charging threshold ±250mV.

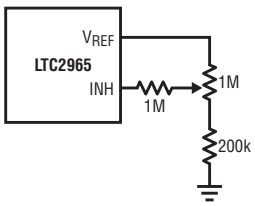


**Figure 3. ±250mV trim scheme. Add to $V_{REF}$ and INH pins in Figure 2.**

While solar panels are normally directed to collect maximum total energy per annum, a standalone system must be optimized for operation under conditions of minimum seasonal insolation, with allowance made for coincidental weather patterns. The primary concern is solar panel orientation, which is a science unto itself. Calculation of a theoretically ideal, fixed orientation is relatively straightforward; nevertheless a host of non-idealities including atmospheric scattering, fog, clouds, shading, horizon angles and other factors make this science inexact, at best. An excellent overview of this subject may be found at www.solarpaneltilt.com. ■

# Powering a Dust Mote from a Piezoelectric Transducer

**Jim Drew**

Increasing the level of remote monitoring and control of industrial environments—such as factories, plants and refineries—enables process engineers and managers to see the overall health of a system or factory, ultimately improving decision making. The easiest way to increase monitoring and control coverage is to use Dust Networks® SmartMesh® wireless sensor networks, which enable easy installation in remote environments. SmartMesh sensors and controllers are often deployed in locations where electrical power connections are not readily available. For this reason, using energy harvesting technology as the source for powering these sensors is attractive.

The LTC3330 is a nanopower buck-boost DC/DC with energy harvesting battery life extender technology that can be attached to a piezoelectric transducer to provide energy to power a Dust Networks mote. The LTC3330 integrates a high voltage step-down energy harvesting power supply plus a buck-boost DC/DC converter powered by a primary cell battery to create a single output always-on power supply that sources power for the remote Dust mote.

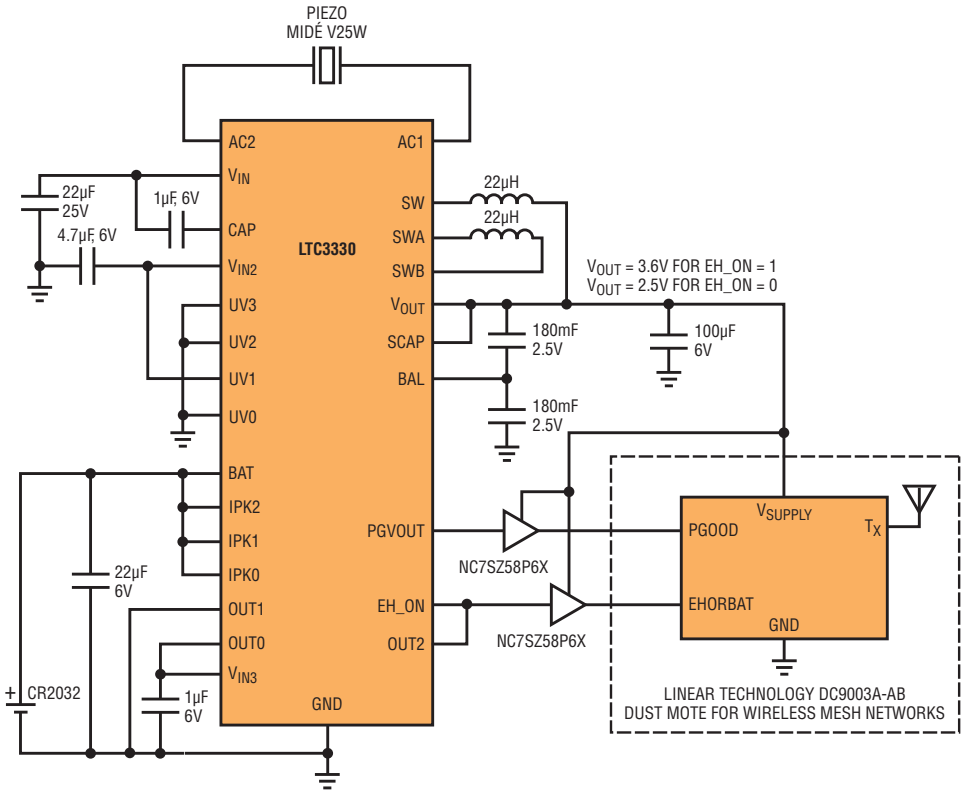


Figure 1. Dust mote setup with a supercapacitor, a battery and EH_ON connected to OUT2

When vibration energy is available, the LTC3330 uses this as its source of power rather than the battery. For short periods when vibration energy isn't available, the LTC3330 charges and balances a supercapacitor that can be called on to support the load. The LTC3330's combination of energy harvesting and supercapacitor charging/balancing circuitry can extend the life of the primary cell battery by several orders of magnitude, resulting in significantly fewer maintenance calls to replace batteries (with the savings multiplied by the number of installed sensors/controllers).

## INTERFACING THE LTC3330 WITH THE DUST MOTE

Figure 1 shows the LTC3330 with an output supercapacitor, a Dust mote attached, a battery installed and EH_ON connected to OUT2. In this configuration, when EH_ON is low, $V_{OUT}$ is set to 2.5V and when EH_ON is high, $V_{OUT}$ is set to 3.6V. A Midé V25W piezoelectric transducer is mechanically attached to a vibration source, and its electrical contacts are connected to the AC1 and AC2 pins of the LTC3330. The vibration source produces $1g_{RMS}$ of force at a 60Hz acceleration, which produces

an open circuit voltage of 10.6$V_{PEAK}$. Figure 2 shows the input capacitor being recharged from the V25W piezoelectric transducer. The input capacitor charges from 4.48V to 5.92V in 208ms. The power delivered from the V25W is 648µW.

The 22µF capacitor is only 18µF at the applied voltage of 5.0V, so every VIN_UVLO_RISING and FALLING event produces 26µC of charge that can be transferred to the output minus the efficiency (90%) of the buck regulator within the LTC3330. Figure 3 shows the charging of the output supercapacitor to 3.6V with the Midé V25W transducer. It takes approximately 3300 seconds for the output supercapacitor to charge to 3.6V.

In Figure 1, when EH_ON is low, $V_{OUT}$ is set to 2.5V and when EH_ON is high, $V_{OUT}$ is set to 3.6V. The first marker in Figure 4 indicates where the vibration source is activated; $V_{IN}$ rises above the VIN_UVLO_RISING threshold. EH_ON goes high causing $V_{OUT}$ to rise toward 3.6V ($V_{OUT}$ starts at 2.5V because the battery has charge). As EH_ON goes high, PGVOUT goes low, since the new $V_{OUT}$ level of 3.6V is not yet reached. As the charge on $V_{IN}$ is transferred to $V_{OUT}$, $V_{IN}$ discharges and when $V_{IN}$ reaches its UVLO_FALLING threshold, EH_ON goes low, causing the targeted $V_{OUT}$ to again be 2.5V.

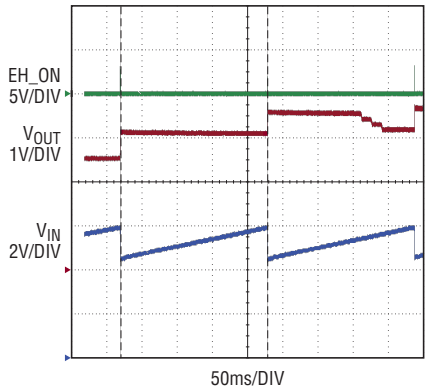


$$P_{C(IN)} = \frac{C_{IN} \bullet \left(V_{IN1}^2 - V_{IN2}^2\right)}{2 \bullet \Delta t} = \frac{18\mu F \bullet \left(5.92^2 - 4.48^2\right)}{2 \bullet 208ms} = 648\mu W$$

Figure 2. Midé V25W charging the 18µF input capacitance from 4.48V to 5.92V in 208ms

Given that the output capacitor is very large and the average load is less than the input power supplied by the Midé piezoelectric transducer, the output voltage increases to the higher set point of 3.6V over many cycles. During the transition from the BAT set point of 2.5V to the energy harvester set point of 3.6V, $V_{OUT}$ is above the 2.5V PGVOUT threshold, hence, PGVOUT goes high every time EH_ON goes low. This cycle repeats until $V_{OUT}$ reaches the PGVOUT threshold for the $V_{OUT}$ setting of 3.6V.

Figure 5 shows the discharging of $V_{OUT}$ when the vibration source is removed and $V_{IN}$ drops below the UVLO_FALLING threshold causing EH_ON to go low. The supercapacitor on $V_{OUT}$ will discharge down to the new target voltage of 2.5V at which point the buck-boost regulator will turn on supplying power to the Dust mote. The discharging of the supercapacitor on $V_{OUT}$ provides an energy source for short-term loss of the vibration source and extends the life of the battery.

## CONCLUSION

The LTC3330 provides a complete solution for powering a Dust Networks mote from a vibration source using the Midé V25W piezoelectric transducer and a primary cell battery connected to the BAT pin. The V25W piezoelectric transducer supports output power requirements from a vibration source, thus extending the life of the battery. When combined with a supercapacitor attached to $V_{OUT}$, the LTC3330 enables even longer extended battery life, reducing maintenance calls to replace batteries. ■

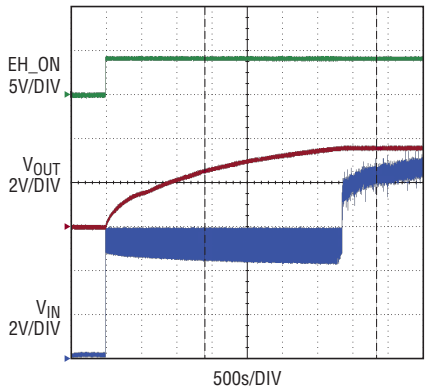


Figure 3. Midé 25W charging output supercapacitor to 3.6V

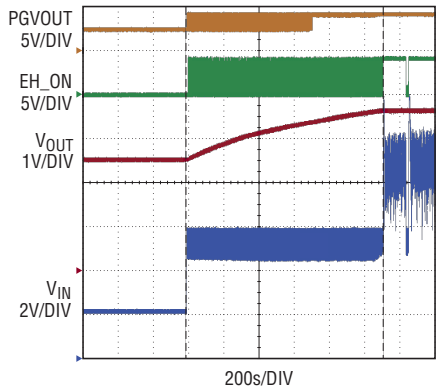


Figure 4. Midé 25W charging output supercapacitor from 2.5V to 3.6V

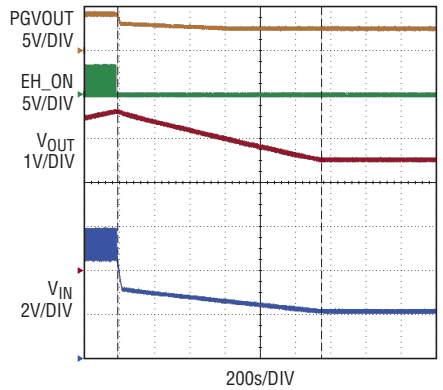


Figure 5. Output supercapacitor discharging when the vibration source is switched off

# New Product Briefs

### 42V, 6A OUTPUT, SYNCHRONOUS STEP-DOWN REGULATOR WITH INTEGRATED CURRENT SENSING

The LT8613 is a 6A, 42V input-capable synchronous step-down switching regulator with integrated current sensing. Synchronous rectification delivers efficiency as high as 95% while Burst Mode® operation keeps quiescent current under 3µA in no load standby conditions. Its 3.4V to 42V input voltage range makes it ideal for automotive and industrial applications. Its internal high efficiency switches deliver up to 6A of continuous output current to voltages as low as 0.97V. An internal current sense amplifier with monitor and control pins enable accurate input or output current regulation and limiting.

The LT8613's Burst Mode operation offers ultralow quiescent current, making it well suited for applications such as automotive always-on systems. The LT8613's unique design maintains a minimum dropout voltage of only 250mV at 3A under all conditions, enabling it to excel in scenarios such as automotive cold crank. Furthermore, a fast minimum on time of only 40ns enables 2MHz constant frequency switching from a 16V input to a 1.5V output, enabling designers to optimize efficiency while avoiding critical noise sensitive frequency bands. The LT8613's 28-lead 3mm × 6mm QFN package and high switching frequency keeps external inductors and capacitors small, providing a compact, thermally efficient footprint.

### NEGATIVE INPUT (–4.5V TO –80V) SYNCHRONOUS BUCK-BOOST/ INVERTING DC/DC CONTROLLER DELIVERS UP TO 20A OUTPUT CURRENT

The LT8709 is a synchronous PWM controller for negative-to-negative or negative-to-positive DC/DC conversion. The LT8709 is unique in solving the problem of regulating a negative voltage with respect to system ground, without the need of complicated level shifting circuitry. The device's synchronous operation means that the output diode is replaced with a high efficiency p-channel MOSFET, thereby increasing efficiency, allowing for higher output currents (up to 20A), and eliminating the heat sink typically required in medium to high power applications. The LT8709 can be configured in buck, boost, buck-boost, and inverting topologies, making it highly versatile for a wide range of power supply designs.

The LT8709 operates over a –4.5V to –80V input voltage range and produces an output voltage from –0.1V to as high as 60V or from –1.4V to as low as –80V. Its rail-to-rail output current monitor and control enables the device to be configured as a current source. The LT8709 features innovative EN/FBIN pin circuitry for slowly varying input signals and an adjustable undervoltage lockout function. This pin is also used for input voltage regulation to avoid collapsing a high impedance supply.

The fixed operating frequency is selectable from 100kHz to 750kHz and can be synchronized to an external clock. Current mode control provides excellent line and load regulation. The LT8709 is configurable for either forced continuous or pulse-skipping operating modes during light load conditions. Additional features include a power good indicator, thermal shutdown and integrated soft-start circuitry.

### 60V/4A & 36V/8A BUCK-BOOST µMODULE REGULATORS IN 15mm × 15mm BGA PACKAGE

The LTM8055 and LTM8056 are buck-boost µModule regulators that seamlessly regulate an output voltage equal to, greater or less than the input voltage. Housed in 15mm × 15mm × 4.92mm BGA package, these devices include the inductor, DC/DC regulator, MOSFETs and the supporting components. The LTM8055 operates from input voltages ranging from 5V to 36V, delivering a load current up to 8A. The LTM8056 has a higher input voltage, up to 60V with 4A load current capability. The compact solution provided by these devices free up PCB board space in systems such as battery operated devices, industrial control, avionics and solar powered equipment.

For battery charging or precision load current adjustment, both devices enable input and output average current limit setting. Moreover, input and output current can be monitored by measuring voltage on a signal pin. Switching frequency is adjustable from 100kHz to 800kHz, and each device can be synchronized to an external clock frequency from 200kHz to 700kHz. With one resistor, the output voltage can be adjusted from 1.2V to 36V (LTM8055) and 1.2V to 48V (LTM8056). ■

## GAIN OF 11 INSTRUMENTATION AMPLIFIER

The LT6023 is a low power, enhanced slew rate, precision operational amplifier. The proprietary circuit topology of this amplifier gives excellent slew rate at low quiescent power dissipation without compromising precision or settling time. In addition, proprietary input stage circuitry allows the input impedance to remain high during input voltage steps as large as 5V. The combination of precision specs along with fast settling makes this part ideal for MUX applications.

**www.linear.com/solutions/5787**

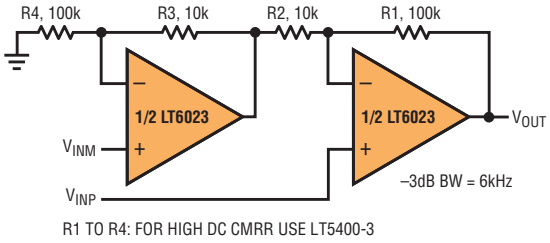


R1 TO R4: FOR HIGH DC CMRR USE LT5400-3

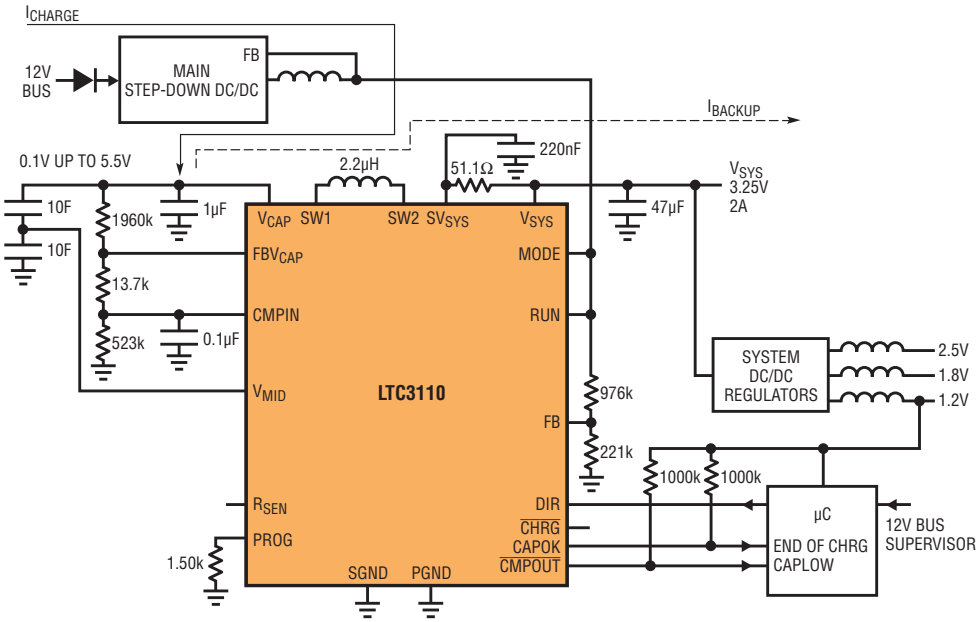


## 2A BIDIRECTIONAL BUCK-BOOST DC/DC REGULATOR AND CHARGER/BALANCER

The LTC3110 is a 2A bidirectional buck-boost DC/DC regulator with capacitor charger and balancer. Its wide 0.1V to 5.5V capacitor/battery voltage and 1.8V to 5.25V system backup voltage ranges make it well suited to a wide variety of backup applications using supercapacitors or batteries. A proprietary low noise switching algorithm optimizes efficiency with capacitor/battery voltages that are above, below or equal to the system output voltage.

**www.linear.com/solutions/5786**

## LT3088 3.3V, 1.6A OUTPUT LINEAR REGULATOR, PARALLEL DEVICES

The LT3088 is an 800mA low dropout linear regulator designed for rugged industrial applications. A key feature of the IC is the extended safe operating area (SOA). The LT3088 can be paralleled for higher output current or heat spreading. The device withstands reverse input and reverse output-to-input voltages without reverse current flow.

**www.linear.com/solutions/5783**

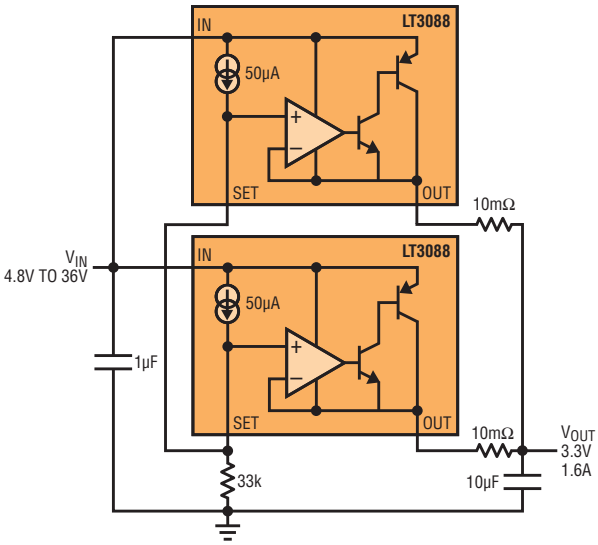


LT, LTC, LTM, Linear Technology, the Linear logo, Burst Mode, Dust, Dust Networks, LTspice, PolyPhase, SmartMesh and µModule are registered trademarks, and LTP, Hot Swap and SmartMesh IP are trademarks of Linear Technology Corporation. All other trademarks are the property of their respective owners. © 2015 Linear Technology Corporation/Printed in U.S.A./70.5K

**Linear Technology Corporation**
1630 McCarthy Boulevard, Milpitas, CA 95035
(408) 432-1900

www.linear.com

Mixed Sources
Product group from well-managed forests and other controlled sources
www.fsc.org Cert no. SW-COC-001530
© 1996 Forest Stewardship Council